

Optical Properties of Aerosol Emitted from Indoor Biomass Burning Cookstoves

by

Samuel Arthur Whidden

A thesis submitted to the
Department of Chemistry and Biochemistry
Mount Allison University
in partial fulfillment of the requirements for the
Bachelor of Science degree with Honours

April 22, 2023

Abstract

Indoor biomass burning cookstoves are used daily by nearly 3 billion people worldwide and are a significant source of $PM_{2.5}$ globally. Light-absorbing organic carbon (OC), also termed brown carbon (BrC) are found within the $PM_{2.5}$ emitted from such cookstoves and can absorb solar radiation and thus alter Earth's energy balance and affect climate. BrC is estimated to be the 4th most significant climate warming agent however most studies investigating the optical properties of BrC focus on outdoor or open biomass burning. Given that few studies have examined BrC emissions from improved or traditional biomass cookstoves, the optical properties of the corresponding aerosols are not well characterized. Additionally, the effect of different fuel types remains unclear. The objective of this study was to determine whether the cookstove or fuel types impact the optical properties of $PM_{2.5}$ emitted from biomass burning cookstoves and to investigate differences between the two major components of BrC, water-soluble BrC (WS-BrC) and methanol-soluble BrC (MS-BrC). To test this, $PM_{2.5}$ samples were collected onto quartz filters using 20 different fuel-cookstove combinations (in triplicate), with 5 different cookstoves (2 traditional and 3 improved) and 4 different fuel types (2 wood and 2 coal). Absorbance spectra for BrC extracts were gathered using a UV-vis spectrometer and absorption coefficients ($b_{abs,\lambda}$) and mass absorption coefficients (MAC_λ) were calculated for 365 nm as this wavelength is commonly chosen in literature to represent the overall optical properties of BrC. It was determined that on average (considering all fuel types) traditional cookstoves emit MS-BrC with $b_{abs,365}$ 9 times greater than improved cookstoves (percent difference of 161). However, after correcting for the mass of OC, the resulting average MAC_{365} values for traditional and improved cookstoves are similar with the improved stoves having a larger MAC_{365} by a percent difference of only 13.6. The resulting average MAC_{365} values indicate that improved cookstoves (designed to reduce $PM_{2.5}$ emissions) did not significantly alter the light absorptivity of MS-BrC compared to traditional cookstoves. The effect of fuel type was often dependent on the cookstove used however for certain cookstoves wood fuels emitted MS-BrC with larger MAC_{365} compared to coal fuels which is consistent with previous studies. Burning charcoal clumps resulted in the least absorbing MS-BrC (lowest MAC_{365}), regardless of cookstove. WS-BrC $b_{abs,365}$ data suggests that water soluble and methanol soluble components of BrC are impacted differently by certain combustion conditions. Additionally, WS-BrC absorption spectra showed unique spectral features when using wood fuels with certain cookstoves that were not present in the corresponding MS-BrC spectra.

Acknowledgments

I would like to express my deepest gratitude and appreciation to Dr. Jenny P. S. Wong who gave me the amazing opportunity of undertaking this project. Thank you for providing me, as well as all your other students, with consistent and incredible support that is simply unmatched. The dedication you have to your students as well as the effort, energy, and enjoyment you bring to every conversation, meeting, lab, or classroom does not go unrecognized.

I would also like to thank all the members of the W(r)ong group during the summer of 2022 who made my introduction to academic research a fun and comfortable experience. A special thanks to Amelia Williams and Lucas Lynch who were also part of the W(r)ong group during the past 2022–2023 academic year and have been amazing group members, providing plenty of assistance and laughs both in and out of the lab. Additionally, I would like to give a particular appreciation to Brad Isenor who provided me with assistance and direction during the initial stages of this project and taught me the basics regarding software programs involved with data analysis in the study.

Finally, I would like to give my heartfelt appreciation to my family including my father Calvin, my mother Joan, my stepmother Lavada, and my siblings Caroline, Christina, Stuart, and Mitchell. This endeavor would not have been possible without your emotional, informational, physical, and financial support, and for that, I am forever grateful.

Table of Contents

Abstract	ii
Acknowledgments.....	iii
List of Figures	v
List of Appendices	v
1 Introduction	1
1.1 Particulate Pollution and Concern for Health and Climate.....	1
1.2 Composition and Characteristics of PM	1
1.3 Aerosol Optical Properties and Effects on Climate	2
1.4 Effects of PM Human Health.....	4
1.5 PM Emitted from Indoor Biomass Burning.....	4
1.6 Research Objectives.....	7
2 Materials and Methods.....	8
2.1 Burning Events.....	8
2.2 PM _{2.5} Sample Collection.....	9
2.3 Elemental and Organic Carbon Analysis	10
2.4 Sample Preparation for BrC Analysis.....	10
2.5 BrC Absorption Analysis.....	11
3 Results and Discussion.....	13
3.1 Elemental and Organic Carbon Abundance.....	13
3.2 Absorption Coefficients for Methanol–Soluble BrC	14
3.3 Mass Absorption Coefficients for Methanol–Soluble BrC.....	17
3.4 Absorption Coefficients for Water–Soluble BrC.....	19
4 Conclusions and Future Direction.....	23
References.....	25
Appendix.....	34

List of Figures

Figure 1.5.1 Map of annual deaths attributed to HAP	5
Figure 2.2.1 Particulate matter collection set-up.....	9
Figure 2.4.1 Scheme of BrC extraction process.. ..	9
Figure 3.1.1 Mass concentration of OC for all cooking methods.....	13
Figure 3.2.1 b_{abs} spectra of MS-BrC.	14
Figure 3.2.2 b_{abs_365} of MS-BrC emitted from all cooking methods.....	16
Figure 3.3.1 MAC_{365} of MS-BrC for all cooking methods.	18
Figure 3.4.1 b_{abs} spectra of WS- and MS-BrC emitted from same combustion event.	20
Figure 3.4.2 b_{abs_365} of WS-BrC emitted from all cooking methods.....	21
Figure 3.4.3 Relative fractional contribution of WS-BrC and MS-BrC to b_{abs_365}	22

List of Appendices

Figure A1 Mass concentrations of EC and OC for all cooking methods.....	34
Figure A2 Relative mass fractions of EC and OC for all cooking methods.....	34
Table A1 b_{abs} of MS-BrC at several wavelengths for all cooking methods.....	35
Table A1 b_{abs} of WS-BrC at several wavelengths for all cooking methods.....	37

Table of Abbreviations

AAE.....	Absorption Angstrom exponent
ACE.....	African Clean Energy One
b_{abs}	Absorption coefficient
$b_{\text{abs}_{365}}$	Absorption coefficient at 365 nm
BC.....	Black carbon
BrC.....	Brown carbon
EC.....	Elemental carbon
GBD.....	Global Burden of Disease
HAP.....	Household air pollution
IAP.....	Indoor air pollution
MAC.....	Mass absorption coefficient
MAC_{365}	Mass absorption coefficient at 365 nm
MS-BrC.....	Methanol-soluble brown carbon
OC.....	Organic carbon
PAH.....	Polycyclic aromatic hydrocarbons
PM.....	Particulate matter
PM_{10}	Course particulate matter
$PM_{2.5}$	Fine particulate matter
WBT.....	Water Boiling Test
WHO.....	World Health Organization
WSOC.....	Water-soluble organic carbon
WS-BrC.....	Water-soluble brown carbon

1 Introduction

1.1 Particulate Pollution and Concern for Health and Climate

Poor air quality has detrimental impacts on both climate and human health. Particulate matter (PM) refers to suspended liquids and solids which play major roles in two of the most pressing environmental issues: climate change and poor air quality. Inhaling PM can cause severe respiratory and cardiovascular diseases and the Global Burden of Disease (GBD) has accordingly ranked ambient PM as the greatest environmental risk factor for premature death in their latest (2019) report.¹ Additionally, in the same report, compared to all other risk factors, not just environmental risks, the GBD ranked ambient PM as the 7th highest risk factor for premature death², above alcohol and drug use, unsafe water, and poor sanitation. These reports along with years of research assessing the risks associated with ambient PM show the severity of the link between outdoor air pollution and human health.

PM has also been proven to have significant impacts on climate as there are certain components within PM which can influence the formation of clouds and scatter or absorb radiation; thus altering Earth's energy balance and affecting climate.³⁻⁶ The impact of PM on climate will be explored in much greater detail in the following sections. Ultimately, the impact PM has on both human health and climate is largely dependent upon their physical and chemical properties and thus, it is critical to understand the composition and optical properties of PM.

1.2 Composition and Characteristics of PM

PM is not one single air pollutant and exists in many different sizes, and compositions. The size of PM is categorized based on their aerodynamic diameter, for example, PM₁₀ refers to PM with a diameter of less than 10 μm and PM_{2.5} (also known as fine particulate matter) refers to PM with an aerodynamic diameter of less than 2.5 μm . Air quality control and regulation guidelines are put into place across the world based on these different size classifications of PM.^{7,8}

PM consists of several major chemical classes, such as organic compounds, inorganic ions, elemental carbon (EC), metals, nitrates, and sulfates.⁹⁻¹¹ There is a multitude of organic compounds found within PM containing many different functional groups which are generalized

and termed as organic carbon (OC). The chemical composition and properties of PM is heavily dependent on their source, such as the fuel used, location, or combustion conditions.^{12,13}

The emission characteristics (i.e., size, composition, concentration, or optical properties) of PM from outdoor sources are much more understood compared to those from indoor sources, particularly regarding PM emitted from indoor cooking activities such as the use of indoor biomass cookstoves. It has been reported that different sizes and compositions of PM have various physiochemical properties and toxic effects.^{7,11,14} Thus, it is critical to understand the effects of indoor sources on PM characteristics and composition in order to make effective conclusions regarding their impacts on human health and climate.

1.3 Aerosol Optical Properties and Effects on Climate

Aerosol (aerosol and PM will be used interchangeably during this thesis) can disrupt the Earth's energy budget either directly via their interaction with incoming solar radiation such as scattering and absorption, or indirectly through aerosol–cloud interactions.^{15,16} These aerosol–cloud interactions arise from aerosols acting as cloud nuclei, potentially increasing cloud albedo or altering the dimensions of cloud particles.^{16,17} Atmospheric aerosol dominates the uncertainty associated with radiative forcing estimates as a result of our limited understanding of processes that control aerosol concentration, composition, optical properties, and cloud interactions. The following discussion will focus on aerosol optical properties as the main focus of this thesis is regarding the light absorptivity of aerosol, specifically PM_{2.5}, emitted from biomass burning cookstoves.

The radiative forcing ability of aerosol depends on their size and composition, however most fine aerosol (PM_{2.5}) scatter incoming solar radiation regardless of their composition.^{18–20} For this reason, PM_{2.5} is often a central focus of studies investigating the optical properties and radiative forcing of atmospheric aerosol. In addition to scattering, light absorbing carbonaceous aerosols such as black carbon (BC) and brown carbon (BrC) can also absorb radiation, warming the surrounding atmosphere.^{19,20} BC, commonly called soot, is a major component within PM_{2.5} and is the third largest positive radiative forcing agent, behind carbon dioxide and methane.²¹ A positive radiative forcing refers to an offset in Earth's energy balance where there is a warming effect as a result of less energy being released back into space compared to what had entered Earth's atmosphere. Some atmospheric aerosols can reflect solar radiation (i.e., via increasing

cloud albedo) and thus have a cooling effect. However, BC and BrC are both dark colored aerosols and so they tend to not have cooling effects. Furthermore, both BC and BrC can deposit onto snow and ice, decreasing albedo and accelerate the melting of glaciers.^{22–24} The past two decades have seen an increasing amount of interest surrounding the climate effects of PM_{2.5}, particularly concerning BC and BrC.^{25,26} BC has been known to be a large contributor to climate change via radiative forcing for many years now.^{25,27,28} BrC refers to the fraction of OC within PM_{2.5} that can absorb light and unlike BC it is only recently being recognized and understood for its impact on climate. In fact, several investigations performed in the past decade have shown that BrC can have a positive radiative forcing ability very similar to that of BC.^{3,6,29–33} Furthermore, carbonaceous aerosols are the main components of PM_{2.5}, contributing to roughly 64% in mass with the OC (BrC) concentration being much higher than that of BC.³⁴ A recent study in Nepal reported a BrC/BC ratio ranging from 2 to 10, further highlighting the dominance of BrC in aerosol composition and the need to further characterize the optical properties of BrC emissions.³⁴

BC and BrC are both primarily generated by the natural and anthropogenic incomplete combustion of fossil fuels, biofuel, and biomass.³⁵ As noted earlier, the composition of PM_{2.5} is heavily dependent on a number of factors surrounding the combustion event, such as the location, source, or fuel. Therefore, in agreement with this understanding, it is known that the light absorption efficiencies of these carbonaceous aerosols are quite variable. The radiative forcing for BrC is still highly uncertain, ranging between +0.03 W/m² and +0.57 W/m², whereas for BC it is much more defined and accepted to be around +0.39 W/m².^{35,36} As these findings show, the radiative forcing and therefore the absorbance capabilities of BrC can vary significantly, sometimes being lower and other times even found to be higher than BC's radiative forcing. Studies suggest that this variation is largely associated with the source, for example, BrC resulting from high temperature combustion tend to be the most absorbing.³⁵ Additionally, the fraction of total aerosol light absorption at the near-UV wavelength attributable to BrC has been reported to be higher for a smoldering combustion compared to a more flaming combustion.²⁸

BrC was previously thought to only absorb significant amounts of light in the short-visible and UV range (i.e., < 400 nm), but it wasn't until recently that it has also been shown to absorb relatively strong in the mid to long visible wavelengths as well (i.e., 400 nm to 600 nm).^{26,29,37,38} In a 2007 study, Sun *et al.* discovered that BrC has two major components, a water-soluble fraction with some UV-Vis absorption, and an organic-soluble fraction with a higher absorption due to

the presence of large molecules with conjugated aromatic rings attached to polar functional groups.³⁹ This organic-soluble (or water-insoluble) fraction is generally evaluated by treating the sample with methanol.⁴⁰ The absorption Angstrom exponent (AAE), along with the mass absorption cross sections (MACs) are important metrics used to evaluate the optical characteristics of carbonaceous aerosol and provides the relative contribution of BrC or BC to the total aerosol absorption. BC is often considered to be the strongest light absorbing carbonaceous aerosol with an AAE of about 1.0, however, the light absorption of BrC is weaker but it exhibits a stronger wavelength dependence.⁴¹ This means that the light absorption efficiency of BrC increases towards short wavelengths more than it does for BC. The studies that found BrC absorbance at longer visible wavelengths noted there was shallower (lower) wavelength dependence associated with this region.^{26,29,37,38} So, although BrC has been recently proven to absorb at these longer visible wavelengths, the light absorbing carbon still absorbs strongest in the short-visible and UV range.

1.4 Effects of PM on Human Health

Numerous epidemiological studies over the past few decades have shown a strong correlation between PM, particularly PM_{2.5}, and severe health effects such as enhanced mortality, cardiovascular, respiratory, and allergic diseases.^{7,13,14} In particular, carbonaceous aerosol contained within PM_{2.5} such as EC and OC have been consistently linked with adverse health effects.^{9,11,27,42} BC and BrC are other classifications of carbonaceous aerosol explored earlier for their impact on climate, however, studies suggest that both of these light absorbing aerosols can also negatively impact human health.^{5,43,44}

1.5 PM Emitted from Indoor Biomass Burning

Outdoor sources of PM_{2.5} have been under investigation for many years and researchers have studied the various effects of this ambient PM on human health and climate in great detail. However, in comparison, little has been done regarding indoor sources. In many countries around the world, most people spend around 80–90% of their time indoors^{45–47} where concentrations of PM have been found to be higher compared to outdoors, especially in developing countries and rural areas.⁴⁸ Considering that we spend a large fraction of our time indoors, it is vital that we understand the various sources of indoor air pollution (IAP) and their corresponding emission characteristics. The primary source of ambient PM_{2.5} is incomplete combustion of fuels from industrial facilities, motor vehicles, fossil fuel power plants, forest fires, and residential burning.

Although some indoor PM_{2.5} can result from outdoor sources, the most prominent source of household air pollution (HAP), especially in rural homes in developing countries, is the residential burning of solid biomass fuels such as wood, charcoal, crop straws, and dung for cooking and heating purposes.⁴⁹ Residential biomass burning is used by nearly 3 billion people worldwide.⁵⁰ Most of the time spent inside by these families is spent in the kitchen nearly adjacent to the stove where the biomass combustion occurs.⁵¹ The WHO states that HAP is the single most important environmental health risk factor worldwide.⁵⁰ In a 2017 report, the GBD stated that globally, incomplete combustion of solid fuels in residential cookstoves leads to severe HAP responsible for about 1.64 million premature deaths.⁵² Figure 1.5.1 shows a map of the world depicting the ranging severity at which countries are affected by HAP resulting from indoor polluting cooking energy.

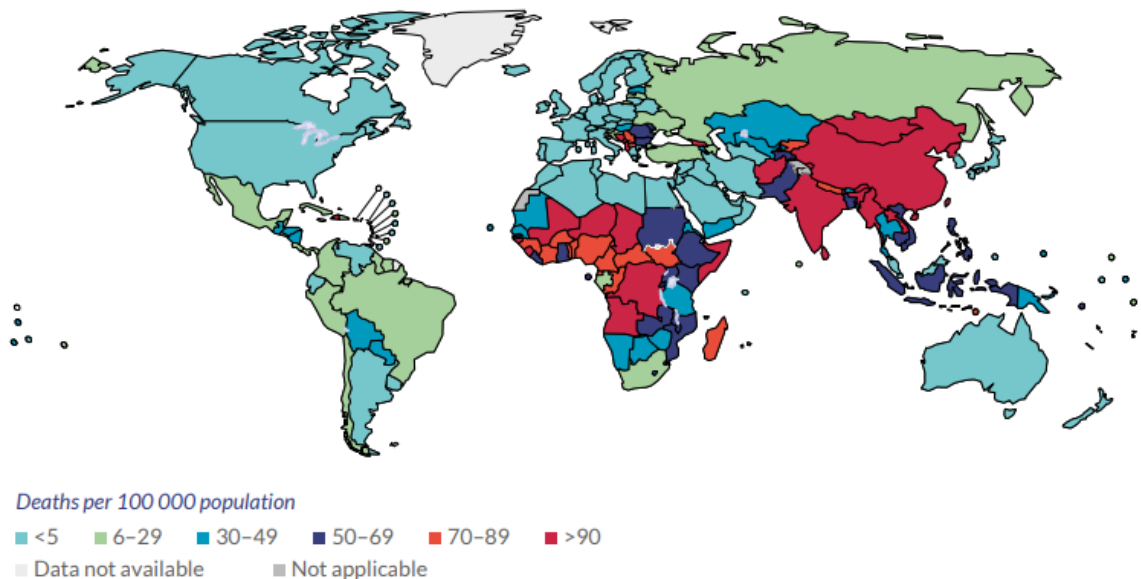


Figure 1.5.1. Deaths per 100,000 population, per year, which are attributable to HAP from polluting cooking energy. Figure obtained from the WHO's Burning Opportunity Report.³⁹

The biomass burning which generates this HAP is often done using traditional cookstoves. The two most common traditional cookstoves used in developing countries are referred to as clay cookstoves and 3-stone cookstoves. Clay cookstoves are U-shaped and are made from clay and the 3-stone cookstove is simply three stones placed opposite to each other in a triangle shape where a pot is then placed on top of the stones. The latter is one of the most widely used cookstoves in developing countries because it is the simplest to create and it is an open fire, allowing for more airflow and therefore less smoldering and overall cleaner combustion compared to the clay

cookstove. However, in most cases, both cookstoves are far from ideal to be used for indoor use and for this reason many organizations, including the WHO, have set out to combat this issue by designing and implementing “improved” cookstoves. Additionally, the United Nations Development Programme have set a goal to have universal access to clean energy cooking by 2030.⁵³ Improved cookstoves are specifically designed to reduce the harmful effects of indoor biomass burning by reducing the amount of PM_{2.5} being emitted from each burning event. Improved cookstoves accomplish this by considering the two factors governing cookstove energy efficiency: combustion efficiency and heat transfer efficiency. Combustion efficiency refers to the ratio of energy released by combustion to the energy in the fuel while heat transfer efficiency refers to the fraction of heat released by combustion that is used in cooking.⁵⁴ Inefficient combustion results in excess fuel use and thus releases more products of incomplete combustion such as particulates including BC, BrC, EC, and OC, which were explored in earlier sections for their climate and health impacts. Traditional cookstoves do very little to control combustion or optimize heat transfer and are therefore highly inefficient in terms of their fuel use.⁵⁴ Improved cookstoves can control these two efficiency factors by optimizing the design of the cookstove. Such design optimizations include, improving the draft available to the fire, implementing a chimney to the stove (typically not one that goes to outside but rather just to provide a larger region for smoke, air, and fire to combine), insulating the fire, or elevating the slot for solid fuel so that air can get underneath the fuel.⁵⁰

Biomass burning has been recognized as a dominant source of BrC across the world. Although many studies have investigated the chemical composition and optical properties of BrC in the atmosphere, only a handful of studies have assessed indoor source emission characteristics of BrC.^{40,41,55–57} One such study was performed by Sun et al. in 2017 where they analyzed the absorbing properties associated with residential coal burning in China and found that BrC accounted for 26.5% of the total absorption, with the other fraction being primarily attributable to BC.⁴¹ However, few studies have focused on the differences in emission of BrC resulting from various fuel–cookstove combinations and therefore the emission characteristics, particularly the optical properties, of the corresponding aerosols are not well characterized.

Understanding PM_{2.5} emitted from indoor biomass burning is also important because it can travel outdoors where previous studies have estimated that in India, nearly 30% of outdoor air pollution

originates from household sources.⁵⁰ The contribution of household sources to outdoor air pollution for other countries still remains unclear.^{58,59}

1.6 Research Objectives

Gaining a better understanding of the chemical composition and physiochemical properties of indoor $PM_{2.5}$ is a fundamental step towards mitigating the negative effects indoor biomass burning has on both human health and climate. Fuel type, cookstove, testing and measurement protocols, and environmental conditions can greatly alter $PM_{2.5}$ emissions, resulting in significant disparities between emission results from the limited existing literature on $PM_{2.5}$ emitted from indoor biomass cookstoves. This makes effective comparisons between current literature challenging which is limiting researchers from further understanding the negative effects of aerosols emitted from such sources. Therefore, it is necessary to understand the emission processes of these air pollutants and how their physiochemical properties and chemical compositions are altered from variations in their combustion conditions (i.e., cookstove or fuel type).

This study aims to address this issue by providing an inventory of $PM_{2.5}$ emission data, containing detailed optical properties of BrC and some preliminary insight towards the chemical composition of $PM_{2.5}$ resulting from 20 different fuel-cookstove combinations. Trends, correlations, and key differences amongst the data will be investigated to try and improve the understanding of how combustion conditions such as fuel type or cookstove can impact the emission characteristics of $PM_{2.5}$ from indoor biomass cookstoves. Due to time constraints, this thesis will focus primarily on the optical properties of $PM_{2.5}$ and investigate MS-BrC and WS-BrC. However, limited and preliminary analysis regarding chemical composition will also be investigated.

Identifying key differences in optical properties between $PM_{2.5}$ emitted from various cookstoves (i.e., improved vs traditional), fuel types (i.e., wood vs charcoal), or sources (i.e., cookstove vs wildfire) will aid in understanding if we should be treating indoor $PM_{2.5}$ emitted from biomass burning differently, depending on source conditions.

2 Materials and Methods

2.1 Burning Events

In this study, PM_{2.5} samples were collected from a variety of burning conditions using 20 different fuel-cookstove combinations. Five different cookstoves (3-stone, clay, EcoZoom Zoom Dura, EcoZoom Zoom Versa, and African Clean Energy One) and four different fuel types (hardwood, softwood pellets, charcoal briquettes, and charcoal clumps) were used. Two of the cookstoves used (3-stone and clay) are referred to as traditional biomass burning cookstoves, whereas the other three are referred to as improved biomass burning cookstoves. The brands of the softwood pellets, charcoal briquettes, and charcoal clumps used were BioGreen, Royal Oak and Sainte Catherine, respectively.

The Water Boiling Test (WBT) protocol is a method used with cookstoves to simulate the cooking process and allow for different types of cookstoves to be compared through a standardized and replicable test.⁶⁰ The WBT protocol followed in this research had three key phases and PM_{2.5} sample collection began in the third phase, referred to as the ‘simmer phase’. This phase required getting the water to simmer at a temperature just below boiling (within 10°C), and once this was achieved, the PM_{2.5} collection began. Throughout the course of the PM_{2.5} collection, the water was kept at a simmer by adding deionized water and fuel as necessary. This simmer phase aims to simulate the long cooking events commonly used throughout the world.⁶⁰ After each burning event, the time spent collecting PM_{2.5} samples, the mass of fuel consumed by the cookstove, the mass of fuel left over, and the mass of ash in the cookstove were all recorded.

2.2 PM_{2.5} Sample Collection



Figure 2.2.1 Experimental set-up for fine particulate matter collection with key instruments and parts labeled. This image features an African Clean Energy One cookstove following the Water Boiling Test protocol (modified image from Isenor, B.H.).

The PM_{2.5} samples were collected using an experimental set-up shown in Figure 2.2.1. The PM_{2.5} sample collection began by drawing up the fumes (aerosol) at a constant flow rate of 18 slpm (maintained using a mass flow controller from Alicat Scientific) through an inlet located right above the cookstove (2–4 cm above) but below the aluminum pot containing the water. Once the aerosol had entered the inlet it was quickly met with a PM_{2.5} cyclone (URG) which was fitted to the inlet and worked to remove any PM larger than 2.5 μm . After the cyclone had selectively allowed only PM with a diameter of 2.5 μm or less to proceed through the system, the flow of aerosol was split into two paths. In each path, the PM_{2.5} was then deposited onto 47 mm quartz filters (heat-treated Tissuquartz Pall Laboratory; pre-collection filter mass was measured using analytical balance) which was contained in a 47 mm filter holder (URG). Both filter holders had two identical 47 mm quartz filters stacked on top of each other. The front filter (first filter in contact with cookstove gas and particle emissions) was used to collect the PM_{2.5} from the burning events while the back filter (directly behind the front filter) was used to collect any gasses or ‘overflow’ of PM from the front filter.^{61,62} The length of PM_{2.5} collection time varied for each burning event as various cookstoves and fuel types had different combustion efficiencies and required a certain length of time to collect a sufficient mass of PM_{2.5} for analysis. Following collection, the weight

of the filters was measured using an analytical balance (Sartorius and BCE124I–1S 0.1 mg accuracy). The PM_{2.5} mass loading (mass of PM_{2.5} per volume of air) were calculated from the difference in the pre- and post-PM collection mass that is normalized by the volume of air that has passed through a given filter (flowrate multiplied by the sample collection time period). After the filter mass was determined, the filters are placed in separate petri-dishes with lids, wrapped in aluminum foil, and stored in sealed bags in a freezer at –35°C until future analysis.

A total of 20 unique fuel-cookstove combinations were tested, using 5 different cookstoves and 4 different fuel types. For each unique fuel-cookstove combination, triplicate PM_{2.5} sampling was performed, providing three filters for each cooking method that came from separate burning events. However, only duplicate sampling was performed for the Clay stove using charcoal briquettes, making for a total of 59 different filters considered in this study.

2.3 Elemental and Organic Carbon Analysis

The organic carbon (OC) and elemental carbon (EC) on the collected quartz filters was analyzed by Sunset Laboratories using an OCEC instrument (Sunset Laboratories),⁶³ following the IMPROVE standardized method.⁶⁴ The reported OC and EC mass per filter area ($\mu\text{g cm}^{-2}$) was normalized to air volume passed through the punch using equation 1,

$$[OC \text{ or } EC]_{norm} = \frac{[OC \text{ or } EC] \times \text{punch size}}{V_{air \text{ through punch}}} \quad (1)$$

where [OC or EC] is the mass concentration per filter area ($\mu\text{g cm}^{-2}$) of OC or EC as reported by Sunset Laboratories, punch size is size of the filter punch used in the BrC analysis, and $V_{air \text{ through punch}}$ is the volume of air (m^3) sampled through the given punch size used for BrC analysis.

2.4 Sample Preparation for BrC Analysis

BrC extraction using water or methanol were performed separately on each filter sample, following the approach by Wong et al.^{65,66} Here, a punch (0.126, 0.283, 1, or 1.5 cm^2) was used to remove a portion of the samples collected on quartz filter and was transferred into a 15 mL centrifuge tube using a sterile pair of forceps. 2.5–5 mL of either deionized water (18.2 m Ω) or methanol (HPLC grade) was added and the tube was sonicated for 1 h to extract the water-soluble (WS-) or methanol-soluble (MS-) BrC. The punch size and volume of water or methanol used was

dependent on how heavily coated the filters were with their collected PM_{2.5} sample, where the resulting extract would result in absorbance values below 2 at 300 nm when analyzed using the UV–VIS spectrophotometer (section 2.5). After sonication, each extract was filtered using a new 0.45 μm PTFE syringe filter (VWR) which was primed with the respective solutions (either 18 mΩ deionized water or methanol). The extract was filtered to remove any insoluble material that can plug the liquid waveguide capillary cell of the UV–VIS spectrophotometer that was used to characterize BrC optical properties (section 2.5). Figure 2.2.2 shows a general scheme of the extraction process.

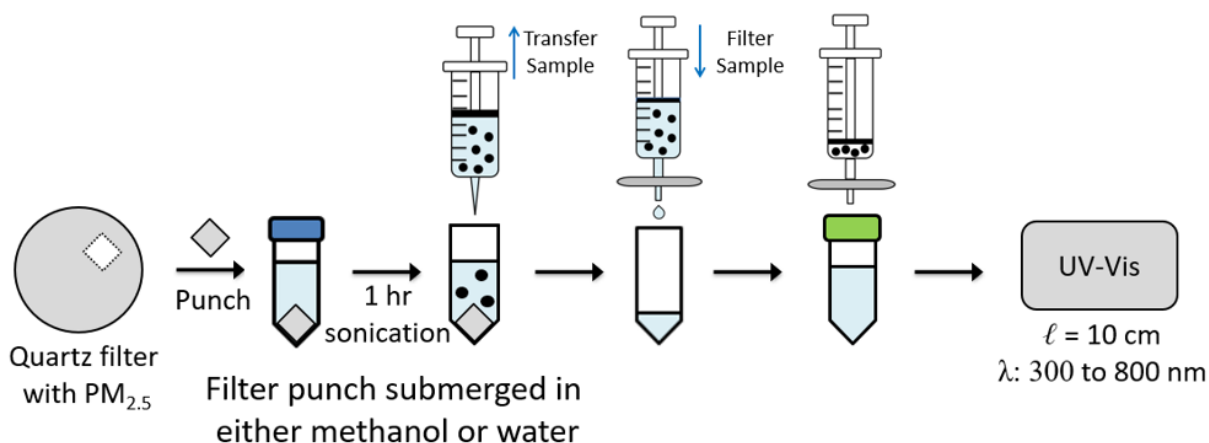


Figure 2.4.1: General scheme of BrC extraction process from filter sample.

2.5 BrC Absorption Analysis

An absorption spectrum (from 300–800 nm) was measured for each of the WS– and MS–BrC extracts using a UV–Vis spectrometer (Ocean Optics USB2000+) and a liquid waveguide capillary cell (LWCC; World Precision Instrument, LWCC–M–10) with a path length of 10 cm, operated using the OceanView software. All absorbance measurements reported herein are solvent (blank containing either water or methanol) corrected. Between each BrC measurement, the LWCC was cleaned by injecting 5 mL of methanol.

To determine the absorption of BrC in air, absorption coefficients ($b_{abs,\lambda}$, units of Mm^{-1}) of BrC at each wavelength were calculated from the measured BrC absorption in solution using the Equation 2:

$$b_{abs,\lambda} = A_{\lambda} \times \left(\frac{V_{ext} \times total\ filter\ area \times \ln 10}{V_a \times punch\ area \times l} \right) \quad (2)$$

where A_λ is the absorbance in solution at a given wavelength; A_{700} is the absorbance in solution at 700 nm; V_{ext} is the volume (mL) of methanol or water used for extraction; V_a is the total volume of air (m^3) sampled during the $\text{PM}_{2.5}$ collection described in section 2.2; the total filter area is the area (cm^2) of the 47 mm quartz filter of which $\text{PM}_{2.5}$ deposited; the punch area was the area (cm^2) of the punch used for the specific filter extraction; and l is the path length (0.1 m). A_{700} was subtracted from A_λ to correct for baseline drift at 700 nm, following the approach of Hecobian et al.⁶⁷ b_{abs_λ} was used as a general measure of BrC as this calculation converts the data from just absorbance to absorption per volume of air, thus allowing an analysis and comparison of the data in meaningful units. The absorption coefficients are commonly used in the BrC literature,^{30,34,40,56,68} and its determination in this work allows comparison to previous studies.

However, absorption coefficients do not consider the mass of BrC present in a given sample. Thus, in order to assess if differences in b_{abs_λ} are due to low OC emissions with high absorptivity or high emissions of OC with low absorptivity, a mass-based absorption coefficient (MAC) is necessary. The MAC_λ for methanol or water extractable light absorbing OC (BrC) was calculated via equation 3.

$$\text{MAC}_\lambda = \frac{b_{\text{abs}_\lambda}}{[\text{OC}]_{\text{norm}}} \quad (3)$$

where $[\text{OC}]_{\text{norm}}$ is the normalized concentration of extracted OC for each filter sample ($\mu\text{g m}^{-3}$) determined from the OC data described in section 2.3.

3 Results and Discussion

3.1 Elemental and Organic Carbon Abundance

The concentration of elemental carbon (EC) and organic carbon (OC) on each filter was determined by Sunset Laboratories and normalized for each burn event using methods described in Section 2.3. The average normalized OC concentrations for all 20 fuel-cookstove combinations are shown in Figure 3.1.1

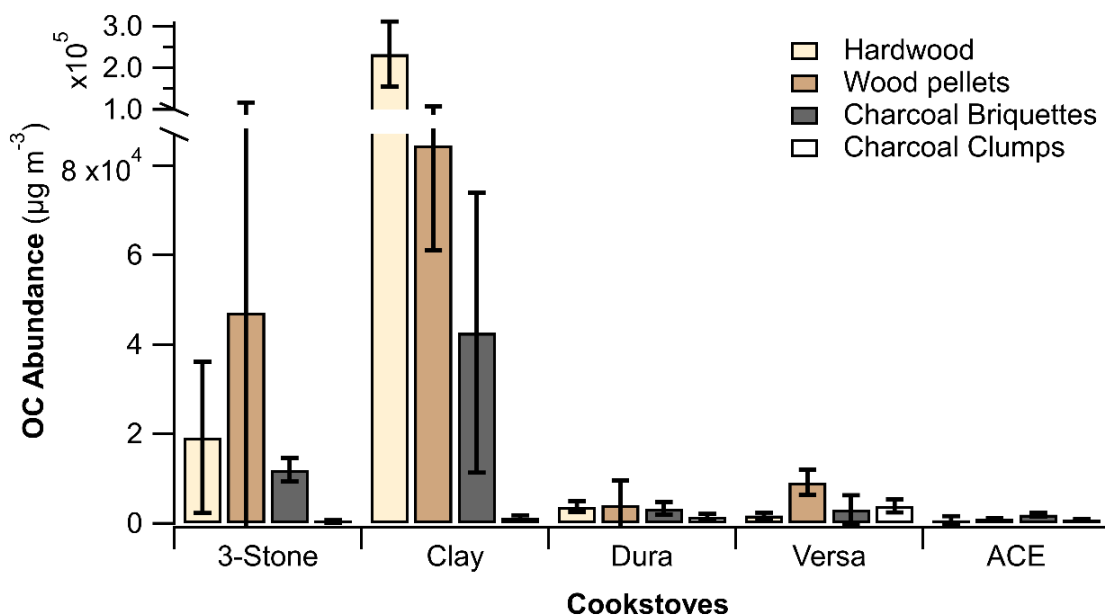


Figure 3.1.1. Average mass concentration of organic carbon ($\mu\text{g m}^{-3}$) for all 20 fuel-cookstove combinations. Error bars represent ± 1 standard deviation ($n=3$).

In general, traditional cookstoves, especially the Clay cookstove, emit larger concentrations of OC compared to improved cookstoves. The collective average for all 8 traditional cookstove cooking methods is $(5.55 \pm 7.22) \times 10^4 \mu\text{g m}^{-3}$ which is 19 times greater than the collective average for the 12 improved cookstove cooking methods ($2.92 \pm 2.21 \times 10^3 \mu\text{g m}^{-3}$). This finding agrees with previous studies that have confirmed reduced $\text{PM}_{2.5}$ emissions from improved cookstoves.⁶⁹ Furthermore, previous work by the Wong group confirmed reduced $\text{PM}_{2.5}$ emissions for improved cookstoves from the same filters used in the current study.⁷⁰

The concentration of EC was not used at any point during analysis however EC are commonly considered in the analysis of optical properties of $\text{BrC}^{34,38,68,71,72}$. Furthermore, EC is commonly used as a surrogate to BC in literature.^{25,41,48,73} Due to a limited time, in-depth analysis on EC was

not carried out for this study. However, preliminary analysis of EC concentrations was performed and the data is presented in Figures A1 and A2. There are some immediate, striking findings from these preliminary comparisons of EC and OC concentration. First, Figure A1 shows that in general, more EC was generated during the use of improved cookstoves compared to traditional cookstoves. This can likely be attributed to the enhanced combustion efficiency of improved cookstoves previously mentioned in section 1.5.⁵⁴ Additionally, Figure A2 shows that PM emitted from the use of coal fuels (briquettes or clumps) is primarily comprised of EC as opposed to OC, regardless of which cookstove is used (exception for ACE and Versa using charcoal briquettes). Furthermore, when using traditional cookstoves, the PM was dominated by OC as opposed to EC regardless of fuel type, whereas for improved cookstoves the fractional composition was dependent on whether wood or coal fuels were burned.

3.2 Absorption Coefficients for Methanol-Soluble BrC

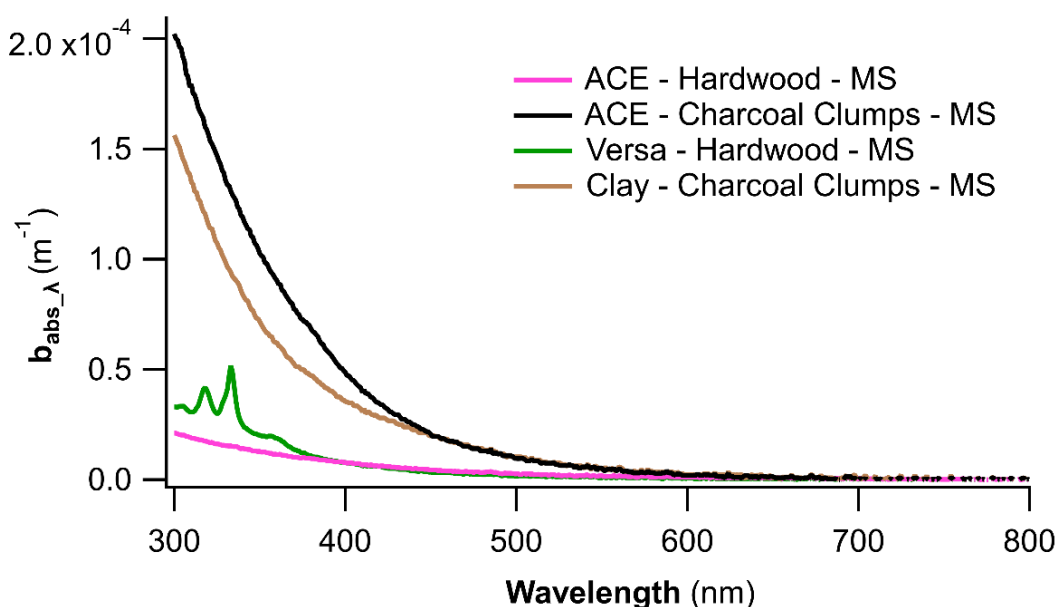


Figure 3.2.1. Absorption coefficient spectra (m^{-1}) of MS-BrC emitted from a selected set of combustion conditions.

A selected set of the absorption coefficient spectra of MS-BrC emitted from different combustion conditions are shown in Figure 3.2.1. The differences in the light absorption spectra for MS-BrC indicates that the combustion conditions (i.e., cookstove or fuel type) significantly influence the absorption properties of MS-BrC. For example, even for the same cookstove, there are clear differences in the shape of the absorption coefficient spectra and the magnitude of the absorption

coefficient from 300 to 600 nm due to the use of different fuels (i.e., ACE using hardwood compared to ACE using charcoal clumps). Similarly, significant differences in the absorption coefficient spectra were observed for MS-BrC emitted from the same fuel but burned using different cookstoves (Versa or ACE using hardwood).

A “smooth” absorption spectrum, such as those from ACE-hardwood, ACE-charcoal clumps, and Clay-charcoal clumps is commonly reported by previous studies.^{68,74} This “smooth” spectral feature is reflective of the chemical complexity of combustion PM_{2.5} as the large number of various compounds should provide a crowded and uniform absorbance at all observed wavelengths. However, burning wood fuel types (hardwood or wood pellets) with the Versa cookstove, resulted in distinct peaks or “spikes” in the absorption spectra around the 300 to 360 nm range (Example shown in Figure 3.2.1). Similar peaks were observed in the same wavelength range for some ACE filters, but only when using wood pellets, meaning that 3 out of the 20 fuel-cookstove combinations resulted in this spectra feature. Similar features for biomass burning aerosols have only been reported once in literature⁶⁸ and suggest that the absorption between 300 to 360 nm is dominated by specific compounds that were only emitted when wood fuels are used with specific cookstoves. Further investigation of these unique spectral features will be discussed in section 3.4.

Due to the large variability of the samples and the challenge to compare 59 different absorption coefficient spectra, only the absorption coefficient at 365 nm ($b_{\text{abs}_{365}}$) is considered for further analysis. 365 nm is commonly chosen as the wavelength of interest within the BrC literature to represent the overall optical properties of BrC.^{34,68,74} This wavelength is chosen for BrC analysis because the majority of OC compounds in PM will absorb strongly at this wavelength.⁷⁴ Furthermore, there is weak absorption at 365 nm from other non-organic compounds in extractions of BrC that could interfere with absorption measurements, making this wavelength optimal for confidently assessing the light absorbance of BrC.³⁴ Additionally, past studies have shown that optical parameters for BrC (i.e., $b_{\text{abs}_{\lambda}}$ and mass-based absorption coefficient, MAC) at 365 nm intercorrelate well with values observed at other wavelengths (e.g., 400, 450, and 500 nm).^{68,75}

Absorption coefficients were also determined for other wavelengths (i.e., 400, 450, 520, 590, and 660 nm) and the averages for all 20 fuel–cookstove combinations are displayed in Table A1.

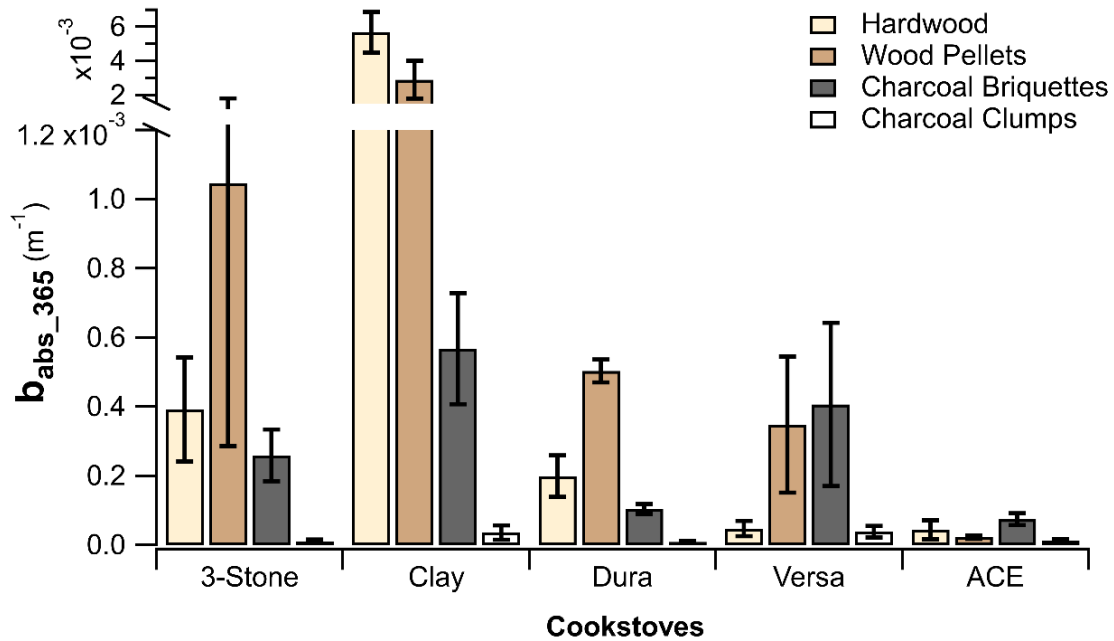


Figure 3.2.2. Average absorption coefficients at 365 nm (m^{-1}) of MS–BrC emitted from all 20 fuel–cookstove combinations. Error bars represent ± 1 standard deviation ($n=3$).

Average $b_{\text{abs}_{365}}$ of MS–BrC emitted from all 20 fuel–cookstove combinations are shown in Figure 3.2.2. The $b_{\text{abs}_{365}}$ for MS–BrC emitted from the Clay stove was extremely variable, spanning $5.7 \times 10^{-3} \text{ m}^{-1}$ to $3.56 \times 10^{-5} \text{ m}^{-1}$. The $b_{\text{abs}_{365}}$ for MS–BrC emitted from charcoal clumps exhibit minimal variability between different cookstoves compared to other fuel types.

The average $b_{\text{abs}_{365}}$ for traditional cookstoves, considering all fuel types (8 cooking methods) was $(1.4 \pm 1.9) \times 10^{-3} \text{ m}^{-1}$ which was 9 times greater than the average for all 12 cooking methods using improved cookstoves ($[1.5 \pm 1.7] \times 10^{-4} \text{ m}^{-1}$). Thus, traditional cookstoves tend to emit MS–BrC with $b_{\text{abs}_{365}}$ that are larger than those from improved cookstoves. Much of this large collective average $b_{\text{abs}_{365}}$ for traditional cookstoves comes from using wood fuels (hardwood or wood pellets) with the Clay cookstove. For example, the average $b_{\text{abs}_{365}}$ for using hardwood fuel with the Clay stove ($[5.7 \pm 1.2] \times 10^{-3} \text{ m}^{-1}$) was 15 times greater than the $b_{\text{abs}_{365}}$ for hardwood with 3–stone ($[3.9 \pm 1.5] \times 10^{-4} \text{ m}^{-1}$).

Moreover, for traditional cookstoves, coal fuels (charcoal briquettes and clumps) emit MS–BrC with lower $b_{\text{abs}_{365}}$ compared to when using wood fuels. Only Dura shares this same relationship

out of all improved cookstoves. When using the Versa or ACE cookstove, charcoal briquettes can result in MS–BrC with an average $b_{\text{abs}_{365}}$ that is equal to or even larger than the $b_{\text{abs}_{365}}$ from using wood fuels.

While absorption coefficients are an important and frequently used proxy for analyzing the light absorption of ambient BrC,^{29,57,76,77} recall that absorption coefficients are not mass corrected (units of m^{-1}) and thus do not consider the mass of BrC present in a given sample. Therefore, a mass absorption coefficient (MAC) is required to assess if the differences in $b_{\text{abs}_{365}}$ are due to the low emissions of OC with high absorptivity (i.e., low mass concentration of OC with large MAC) or high emissions of OC with low absorptivity (i.e., high mass concentration of OC with low MAC).

3.3 Mass Absorption Coefficients for Methanol–Soluble BrC

Mass absorption coefficients (MACs), also referred to as mass absorption efficiency (MAE), are used to describe the absorption efficiency of MS–BrC per mass of OC. As seen on Figure 3.3.1, when considering all fuel types, the average MAC_{365} for the Clay cookstove ($0.025 \pm 0.010 \text{ m}^2 \text{ g}^{-1}$) is the lowest compared to all other cookstoves and additionally has the least variability between different fuel types. Since the Clay cookstove emits the largest amount of OC (Figure 3.1.1) but the MS–BrC is not strongly absorbing per mass of OC compared to emissions from other cookstoves, the large $b_{\text{abs}_{365}}$ for Clay stove is primarily driven by the amount of OC emitted. Collectively, the Clay cookstove results in the highest emissions of OC that is of the lowest light absorptivity amongst all cookstoves tested in this study.

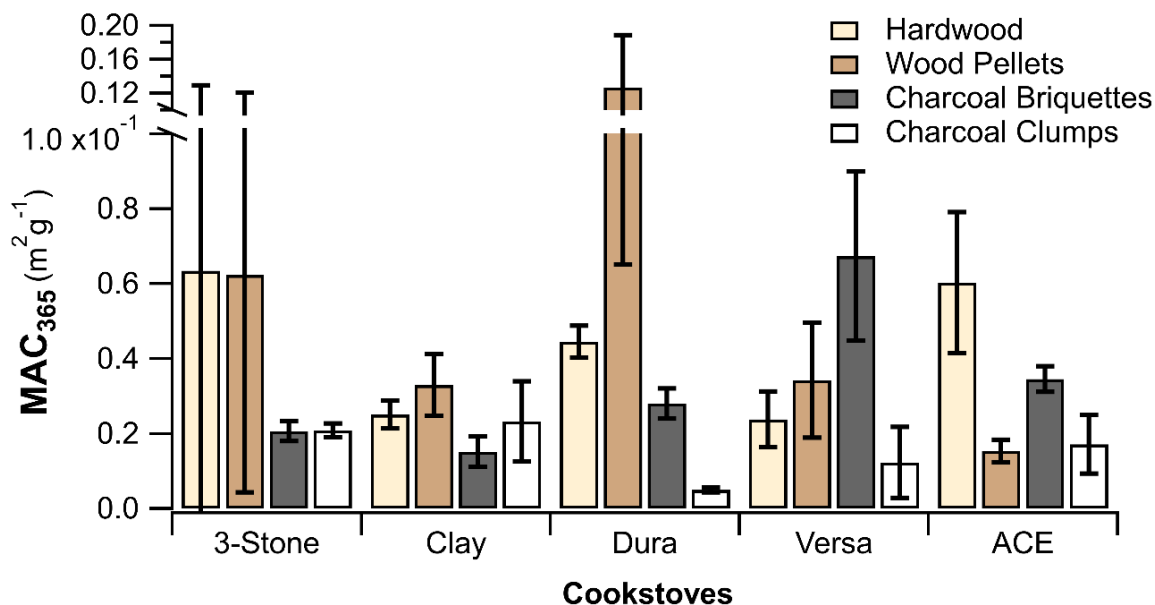


Figure 3.3.1. Average MAC_{365} ($m^2 g^{-1}$) of MS–BrC for all 20 fuel–cookstove combinations. Error bars represent ± 1 standard deviation ($n=3$).

While the improved cookstoves were deployed with the goal to mitigate the adverse human health effects associated with indoor biomass burning,⁶⁹ the average MAC_{365} for improved cookstoves ($0.039 \pm 0.038 m^2 g^{-1}$) are similar to that for traditional cookstoves ($0.034 \pm 0.0037 m^2 g^{-1}$). Indicating that the cookstove type did not significantly alter the light absorptivity of organic MS–chromophore compared to those emitted from traditional cookstoves. In fact, for certain improved cookstoves, burning specific fuels can result in the emission of MS–BrC of higher light absorptivity than traditional cookstoves burning the same fuel. For example, the burning of wood pellets using Dura, an improved cookstove, resulted in the emission of MS–BrC with the highest MAC_{365} ($0.127 \pm 0.062 m^2 g^{-1}$) which is 2 – 4 times higher than the MS–BrC emitted from traditional cookstoves using wood pellets.

The effect of fuel type on the light absorptivity of the MS–BrC (MAC_{365}) was often dependent on the cookstove used and could vary significantly (as previously noted for wood pellets). However, using wood fuels (hardwood or wood pellets) with specific cookstoves (i.e., 3–stone or Dura), resulted in the emission of MS–BrC with larger MAC_{365} compared to using coal fuels (briquettes or clumps), suggesting that certain cookstoves can result in the emission of MS–BrC with higher light absorptivity when burning wood fuels as opposed to coal fuels. This finding is consistent with MAC_{365} of MS–BrC emitted from indoor biomass cookstoves that were reported by one of few other studies performing a similar investigation. Xie *et al.* found wood fuel (red oak) to

generate MS–BrC with MAC_{365} values ($4.20 \pm 2.18 \text{ m}^2 \text{ g}^{-1}$) that were 2 to 6 times greater than the value associated with using charcoal clumps ($1.78 \pm 0.34 \text{ m}^2 \text{ g}^{-1}$).⁶⁸ The cookstoves used in the Xie *et al.* study (1 traditional and 4 improved stoves) ranged from a 3–stone stove to a forced–draft improved cookstove similar to the ACE used in this study. The magnitude of the MAC_{365} values reported by Xie *et al.* are notably larger than the values obtained in this study. However, previous studies have observed large variability in MAC_{365} values for biomass burning BrC which is often attributable to different combustion conditions, instrumentation, and sampling techniques being used for various studies.^{40,65,66,68,71,78,79} For example, MAC_{365} values for wood burning have been reported to vary from 0.02 to $4.20 \text{ m}^2 \text{ g}^{-1}$.^{40,65,66,68,79} The MAC_{365} values observed in this study fell on the lower end of such previously reported ranges.

Figure 3.3.1 also shows that there are two charcoal fuel and improved cookstove combinations (Versa and ACE with charcoal briquettes) that emitted MS–BrC that is more absorbing per mass (larger MAC_{365}) compared to using certain wood fuels, further indicating that wood fuels do not always result in the emission of MS–BrC with higher light absorptivity and that the type of cookstove can also play a significant role.

Figure 3.3.1 highlights that using charcoal clumps as a fuel source emits MS–BrC with the lowest MAC_{365} values amongst all fuel types, regardless of which cookstove is used. This cannot be said for any other fuel source. Thus, charcoal clumps result in the emission of MS–BrC of the lowest light absorptivity due to low emissions of weakly absorbing BrC.

3.4 Absorption Coefficients for Water–Soluble BrC

It is common practice within the literature to separate BrC into WS and MS fractions^{40,41,68,80–82}, as mentioned previously (section 1.3), WS and organic–soluble carbon are the two major components of BrC.³⁹ Breaking the optical properties down into these fractions helps to decouple the data and draw more meaningful conclusions regarding either chemical composition or optical properties.

Something worth noting regarding the WS fraction of BrC emitted from these various combustion events, is how there were some major spectral differences in the absorption coefficients.

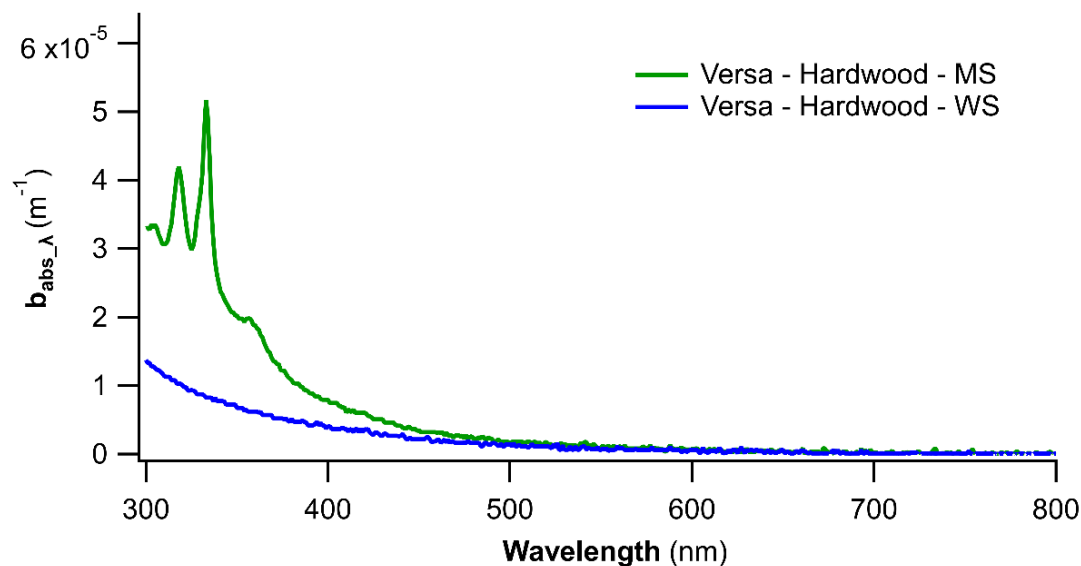


Figure 3.4.1. Absorption coefficient spectra (m^{-1}) for both the water soluble and methanol soluble fractions of BrC resulting from the same combustion event.

The absorption coefficient spectra for MS– and WS–BrC from the Versa stove and hardwood fuel is shown in Figure 3.4.1. For the WS fraction, the unique “spikes” spectral features that occur for the MS–BrC spectra (previously mentioned in Section 3.2) are not present. This was true for all cases where these unique “spikes” were observed in the absorption coefficient spectra of MS–BrC samples (i.e., for Versa–hardwood, Versa–wood pellets, and ACE–wood pellets) are not present for the corresponding WS-BrC absorption coefficient spectra. This observation indicates that the compound(s) are responsible for these peaks in the spectra, are not water soluble and must be at least moderately methanol soluble. Polycyclic aromatic hydrocarbons (PAHs), such as pyrene or benzo[a]pyrene are formed during the incomplete combustion or pyrolysis of organic material^{83–85} (i.e., wood) and are not WS but are moderately MS.⁸⁶ Furthermore, the absorption spectra for both pyrene and benzo[a]pyrene feature an extremely similar “3–pronged” peak in the 300 to 400 nm range^{87,88}, similar to the features observed here in this study. It is possible that these peaks are not observed for any filters using coal fuel because the initial pyrolysis of wood to charcoal could be emitting most of these PAHs, however this needs to be investigated in future studies.

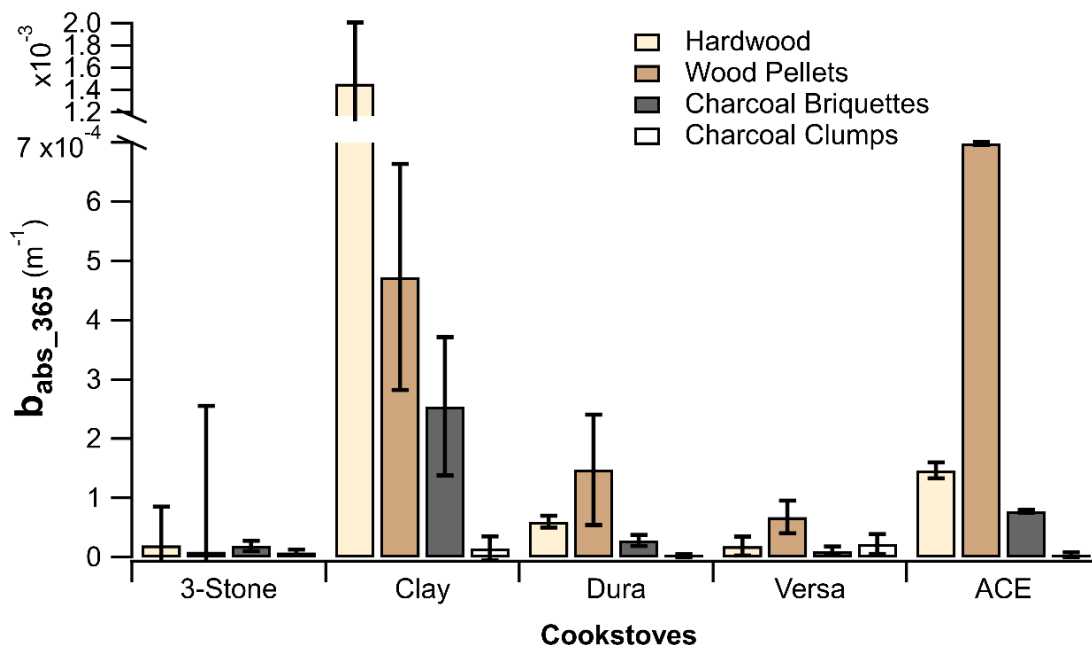


Figure 3.4.2. Average absorption coefficients at 365 nm (m^{-1}) of WS-BrC emitted from all 20 fuel-cookstove combinations. Error bars represent ± 1 standard deviation ($n=3$).

Figure 3.4.2 shows a low variability in b_{abs_365} values for WS-BrC, irrespective of fuel type, for some cookstoves whereas there is a large variability for others (Clay and ACE). This is interesting because for the MS-BrC, the ACE stove emitted BrC with the least variable b_{abs_365} across different fuel types (Figure 3.2.2). This suggests that the light absorptivity of the water-soluble components of BrC emitted when using the ACE cookstove are more influenced by burning different fuels, likely due to variation in combustion conditions, compared to the methanol soluble components. Similarly, the b_{abs_365} of WS-BrC emitted when using the 3-stone stove shows little variability between different fuel types, however the b_{abs_365} of MS-BrC emitted from the 3-stone stove was the second most variable behind the Clay stove, further indicating that the light absorptivity of WS- and MS-BrC fractions can be affected differently by the same cooking methods.

Similar to the MS-BrC b_{abs_365} , the type of cookstove appears to have a larger influence on the b_{abs_365} of WS-BrC when using wood fuels compared to coal fuels which show a low variance between different cookstoves, especially charcoal clumps.

The magnitude of WS-BrC b_{abs_365} were smaller than the corresponding MS-BrC b_{abs_365} values for all 20 fuel-cookstove combinations which is consistent with previous studies.^{39,42,67,81}

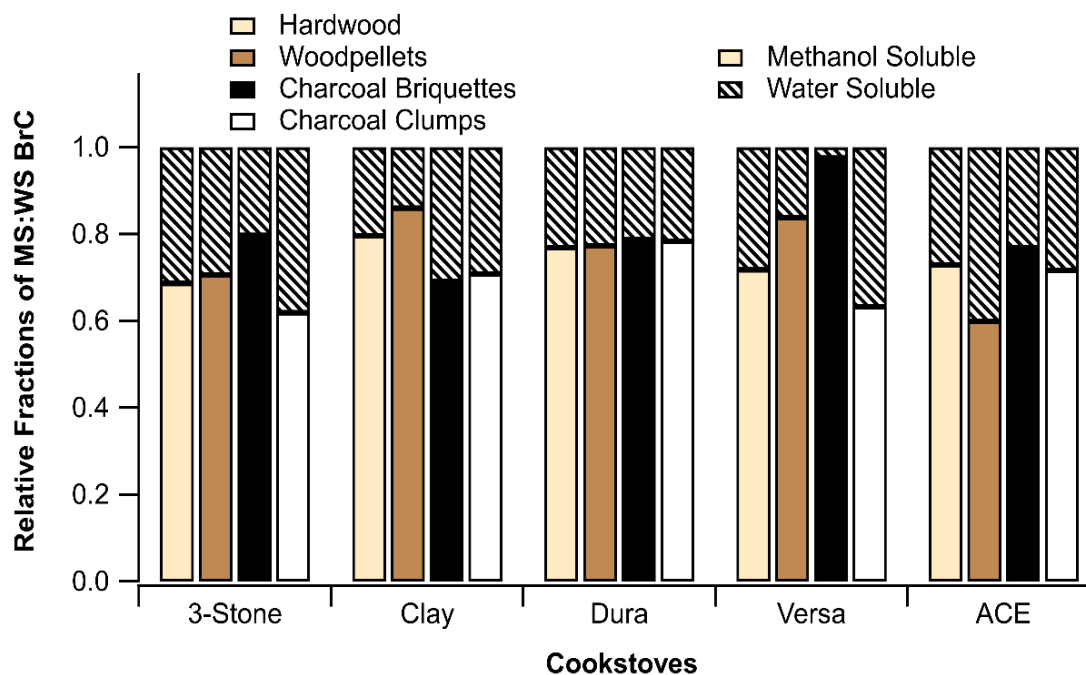


Figure 3.4.3. Relative contribution of WS–BrC (dashed) and MS–BrC (solid) to the $b_{\text{abs}_{365}}$ for all 20 fuel–cookstove combinations.

Figure 3.4.3 shows the relative contribution of WS–BrC and MS–BrC to the overall $b_{\text{abs}_{365}}$ for all 20 unique fuel–cookstove combinations. It can be seen that MS–BrC contributes to the majority of the $b_{\text{abs}_{365}}$ (at least 60%) irrespective of the cookstove or fuel type used. Moreover, WS–BrC can contribute anywhere from as little as 2.5% (Versa + charcoal briquettes) to as much as 40% (ACE + wood pellets) to the total (WS and MS) $b_{\text{abs}_{365}}$. While the contribution of WS– and MS–BrC can be variable for some cookstove types (irrespective of fuels), for the Dura cookstove, the relative contribution of WS– and MS–BrC to total $b_{\text{abs}_{365}}$ remained quite constant (0.77 to 0.79) for all four fuel types. This suggests that the combustion conditions for Dura did not affect the solubility of and the light absorption of BrC emitted.

The relative importance of MS– and WS–BrC to the direct radiative impacts of PM remains unclear, as currently it is unknown whether MS and WS–BrC undergo different atmospheric reactive loss (i.e., photochemical oxidation).^{79,89–91} Thus, having data such as the relative fractional contribution of MS and WS–BrC to $b_{\text{abs}_{365}}$ could help with generating future estimates or models regarding BrC radiative forcing as these two components may have to be considered differently.

Note that MAC values could not be calculated for WS–BrC as it is not known how much of the OC on each filter is water soluble (i.e., water soluble organic carbon, WSOC, was not measured).

4 Conclusions and Future Direction

This study measured the light absorption of MS– and WS–BrC emitted from 20 different cooking methods using two commonly reported metrics within BrC literature for analyzing its optical properties: $b_{\text{abs},365}$ and MAC_{365} . The latter is a mass–based absorption coefficient whereas the former does not account for the mass of BrC present in a given sample. The 20 unique cooking methods were generated using 5 different biomass burning cookstoves (2 traditional and 3 improved) and 4 different fuel types (2 wood and 2 coal). It was determined that on average (considering all fuel types) traditional cookstoves emit MS–BrC with $b_{\text{abs},365}$ 9 times greater than improved cookstoves. However, after correcting for the mass of OC, the resulting average MAC_{365} for traditional and improved cookstoves are similar with the improved stoves having a larger MAC_{365} by a percent difference of only 13.6. This was interesting as it indicates that improved cookstoves (designed to reduce $\text{PM}_{2.5}$ emissions) do not significantly alter the light absorptivity of MS–BrC compared to traditional cookstoves. In fact, burning specific fuels in certain improved cookstoves resulted in MS–BrC of higher light absorptivity than traditional cookstoves burning the same fuel.

For certain cookstoves, wood fuels emitted MS–BrC with larger MAC_{365} compared to using coal fuels which is consistent with previous studies, suggesting a relationship where wood fuels result in MS–BrC of higher light absorptivity. Burning charcoal clumps resulted in the least absorbing MS–BrC (lowest MAC_{365}), regardless of cookstove.

WS–BrC $b_{\text{abs},365}$ data suggests that water soluble and methanol soluble components of BrC are impacted differently by certain combustion conditions. Additionally, WS–BrC absorption spectra showed unique spectral features when using wood fuels with certain cookstoves that have not been reported in literature. Further analysis and composition characterization is required in order to confidently identify the root of these unique spectral features that have not been reported in the literature. However, the preliminary analysis performed in this study is a step in the right direction and will help to narrow down the techniques and further analysis necessary to characterize the chemical composition of these unique filters in the future. For example, characterization of the

organic carbon using GC–MS, and FT–IR could be used to identify the specific PAHs, and functional groups associated with the BrC.

In terms of other future directions with this project, if WSOC can be determined and MAC_{365} values are calculated, it would be of interest to make a similar plot to Figure 3.3.1 for WS–BrC so that the data and trends could be compared to that of the MS–BrC. Additionally, a similar fractional contribution graph to Figure 3.4.2 for MAC_{365} data would be useful for the same reason. Additionally, further consideration of the mass concentrations of EC or BC mentioned in section 3.1.1 and showed in Figures A1 and A2 could provide a wider and more detailed understanding towards light absorptivity of carbonaceous aerosols emitted from these indoor combustion events. As previously alluded to in section 3.4, the exact atmospheric reactive loss of MS– and WS–BrC still remains unclear and so investigating that would aid in making use of the relative fractional contribution of MS– and WS–BrC to $b_{abs,365}$ as well as the similar plot for MAC_{365} which should be made in the future. Lastly, it would be of interest to perform correlative analysis on the physiochemical properties as well as EC and OC concentrations of cookstove aerosols observed here to DTT toxicity previously characterized by a previous member of the Wong group on the same filters⁷⁰, as previous work has suggested that BrC is well correlated with DTT activity.⁹²

With the results of this study, we have provided a dataset that can be used for further investigations regarding the optical properties of BrC emitted from indoor biomass burning cookstoves. We hope that this preliminary analysis towards how cookstove and fuel types can impact the optical properties of $PM_{2.5}$ can facilitate a greater understanding of the absorption capabilities of aerosol emitted from such sources, as current literature and understandings are limited.

References

- (1) Bennitt, F. B.; Wozniak, S. S.; Causey, K.; Burkart, K.; Brauer, M. Estimating Disease Burden Attributable to Household Air Pollution: New Methods within the Global Burden of Disease Study. *The Lancet Global Health* **2021**, *9*, S18.
- (2) GBD 2019 Viewpoint Collaborators. Five Insights from the Global Burden of Disease Study 2019. *Lancet* **2020**, *396* (10258), 1135–1159.
- (3) Lin, G.; Penner, J. E.; Flanner, M. G.; Sillman, S.; Xu, L.; Zhou, C. Radiative Forcing of Organic Aerosol in the Atmosphere and on Snow: Effects of SOA and Brown Carbon. *Journal of Geophysical Research: Atmospheres* **2014**, *119* (12), 7453–7476.
- (4) Shen, G.; Tao, S.; Wei, S.; Zhang, Y.; Wang, R.; Wang, B.; Li, W.; Shen, H.; Huang, Y.; Chen, Y.; Chen, H.; Yang, Y.; Wang, W.; Wei, W.; Wang, X.; Liu, W.; Wang, X.; Simonich, S. L. M. Reductions in Emissions of Carbonaceous Particulate Matter and Polycyclic Aromatic Hydrocarbons from Combustion of Biomass Pellets in Comparison with Raw Fuel Burning. *Environ Sci Technol* **2012**, *46* (11), 6409–6416.
- (5) Pöschl, U. Aerosol Particle Analysis: Challenges and Progress. *Anal Bioanal Chem* **2003**, *375* (1), 30–32.
- (6) Saleh, R.; Marks, M.; Heo, J.; Adams, P. J.; Donahue, N. M.; Robinson, A. L. Contribution of Brown Carbon and Lensing to the Direct Radiative Effect of Carbonaceous Aerosols from Biomass and Biofuel Burning Emissions. *Journal of Geophysical Research: Atmospheres* **2015**, *120* (19), 10,285–10,296.
- (7) Yin, P.; Guo, J.; Wang, L.; Fan, W.; Lu, F.; Guo, M.; Moreno, S. B. R.; Wang, Y.; Wang, H.; Zhou, M.; Dong, Z. Higher Risk of Cardiovascular Disease Associated with Smaller Size-Fractioned Particulate Matter. *Environ. Sci. Technol. Lett.* **2020**, *7* (2), 95–101.
- (8) Nazarenko, Y.; Pal, D.; Ariya, P. A. Air Quality Standards for the Concentration of Particulate Matter 2.5, Global Descriptive Analysis. *Bull World Health Organ* **2021**, *99* (2), 125–137D.
- (9) Wang, J.; Yu, A.; Yang, L.; Fang, C. Research on Organic Carbon and Elemental Carbon Distribution Characteristics and Their Influence on Fine Particulate Matter (PM_{2.5}) in Changchun City. *Environments* **2019**, *6* (2), 21.
- (10) Anderson, J. O.; Thundiyil, J. G.; Stolbach, A. Clearing the Air: A Review of the Effects of Particulate Matter Air Pollution on Human Health. *J. Med. Toxicol.* **2012**, *8* (2), 166–175.
- (11) Rappazzo, K. M.; Daniels, J. L.; Messer, L. C.; Poole, C.; Lobdell, D. T. Exposure to Elemental Carbon, Organic Carbon, Nitrate, and Sulfate Fractions of Fine Particulate Matter and Risk of Preterm Birth in New Jersey, Ohio, and Pennsylvania (2000–2005). *Environ Health Perspect* **2015**, *123* (10), 1059–1065.

- (12) McMurry, P. H.; Shepherd, M. F.; Vickery, J. S. *Particulate Matter Science for Policy Makers: A NARSTO Assessment*; Cambridge University Press, 2004.
- (13) Pöschl, U. Atmospheric Aerosols: Composition, Transformation, Climate and Health Effects. *Angewandte Chemie International Edition* **2005**, *44* (46), 7520–7540.
- (14) Achilleos, S.; Kioumourtzoglou, M.-A.; Wu, C.-D.; Schwartz, J. D.; Koutrakis, P.; Papatheodorou, S. I. Acute Effects of Fine Particulate Matter Constituents on Mortality: A Systematic Review and Meta-Regression Analysis. *Environment International* **2017**, *109*, 89–100.
- (15) Steiner, A. L.; Mermelstein, D.; Cheng, S. J.; Twine, T. E.; Oliphant, A. Observed Impact of Atmospheric Aerosols on the Surface Energy Budget. *Earth Interactions* **2013**, *17* (14), 1–22.
- (16) Mushtaq, Z.; Sharma, M.; Bangotra, P.; Gautam, A. S.; Gautam, S. Atmospheric Aerosols: Some Highlights and Highlighters, Past to Recent Years. *Aerosol Science and Engineering* **2022**, *6* (2), 135–145.
- (17) Haywood, J. M.; Abel, S. J.; Barrett, P. A.; Bellouin, N.; Blyth, A.; Bower, K. N.; Brooks, M.; Carslaw, K.; Che, H.; Coe, H.; Cotterell, M. I.; Crawford, I.; Cui, Z.; Davies, N.; Dingley, B.; Field, P.; Formenti, P.; Gordon, H.; de Graaf, M.; Herbert, R.; Johnson, B.; Jones, A. C.; Langridge, J. M.; Malavelle, F.; Partridge, D. G.; Peers, F.; Redemann, J.; Stier, P.; Szpek, K.; Taylor, J. W.; Watson-Parris, D.; Wood, R.; Wu, H.; Zuidema, P. The CLOUD–Aerosol–Radiation Interaction and Forcing: Year 2017 (CLARIFY-2017) Measurement Campaign. *Atmospheric Chemistry and Physics* **2021**, *21* (2), 1049–1084.
- (18) Forster, P., V. Ramaswamy, P. Artaxo, T. Berntsen, R. Betts, D.W. Fahey, J. Haywood, J. Lean, D.C. Lowe, G. Myhre, J. Nganga, R. Prinn, G. Raga, M. Schulz and R. Van Dorland, 2007: Changes in Atmospheric Constituents and in Radiative Forcing. In: *Climate Change 2007: The Physical Science Basis. Contribution of Working Group I to the Fourth Assessment Report of the Intergovernmental Panel on Climate Change* [Solomon, S., D. Qin, M. Manning, Z. Chen, M. Marquis, K.B. Averyt, M. Tignor and H.L. Miller (eds.)]. Cambridge University Press, Cambridge, United Kingdom and New York, NY, USA
- (19) Schwartz, S. E. The Whitehouse Effect—Shortwave Radiative Forcing of Climate by Anthropogenic Aerosols: An Overview. *Journal of Aerosol Science* **1996**, *27* (3), 359–382.
- (20) Péré, J. C.; Mallet, M.; Pont, V.; Bessagnet, B. Impact of Aerosol Direct Radiative Forcing on the Radiative Budget, Surface Heat Fluxes, and Atmospheric Dynamics during the Heat Wave of Summer 2003 over Western Europe: A Modeling Study. *Journal of Geophysical Research: Atmospheres* **2011**, *116* (D23).
- (21) Sato, M.; Hansen, J.; Koch, D.; Lacis, A.; Ruedy, R.; Dubovik, O.; Holben, B.; Chin, M.; Novakov, T. Global Atmospheric Black Carbon Inferred from AERONET. *Proc Natl Acad Sci U S A* **2003**, *100* (11), 6319–6324.

- (22) Wu, G.-M.; Cong, Z.-Y.; Kang, S.-C.; Kawamura, K.; Fu, P.-Q.; Zhang, Y.-L.; Wan, X.; Gao, S.-P.; Liu, B. Brown Carbon in the Cryosphere: Current Knowledge and Perspective. *Advances in Climate Change Research* **2016**, *7* (1), 82–89.
- (23) Kang, S.; Zhang, Y.; Qian, Y.; Wang, H. A Review of Black Carbon in Snow and Ice and Its Impact on the Cryosphere. *Earth-Science Reviews* **2020**, *210*, 103346.
- (24) Beres, N. D.; Sengupta, D.; Samburova, V.; Khlystov, A. Y.; Moosmüller, H. Deposition of Brown Carbon onto Snow: Changes in Snow Optical and Radiative Properties. *Atmospheric Chemistry and Physics* **2020**, *20* (10), 6095–6114.
- (25) Andreae, M. O.; Gelencsér, A. Black Carbon or Brown Carbon? The Nature of Light-Absorbing Carbonaceous Aerosols. *Atmospheric Chemistry and Physics* **2006**, *6* (10), 3131–3148.
- (26) Saleh, R.; Robinson, E. S.; Tkacik, D. S.; Ahern, A. T.; Liu, S.; Aiken, A. C.; Sullivan, R. C.; Presto, A. A.; Dubey, M. K.; Yokelson, R. J.; Donahue, N. M.; Robinson, A. L. Brownness of Organics in Aerosols from Biomass Burning Linked to Their Black Carbon Content. *Nature Geosci* **2014**, *7* (9), 647–650.
- (27) Magalhaes, S.; Baumgartner, J.; Weichenthal, S. Impacts of Exposure to Black Carbon, Elemental Carbon, and Ultrafine Particles from Indoor and Outdoor Sources on Blood Pressure in Adults: A Review of Epidemiological Evidence. *Environ Res* **2018**, *161*, 345–353.
- (28) Holder, A. L.; Hagler, G. S. W.; Aurell, J.; Hays, M. D.; Gullett, B. K. Particulate Matter and Black Carbon Optical Properties and Emission Factors from Prescribed Fires in the Southeastern United States: Aerosol Optical Properties from Fires. *J. Geophys. Res. Atmos.* **2016**, *121* (7), 3465–3483.
- (29) Hoffer, A.; Tóth, Á.; Pósfai, M.; Chung, C. E.; Gelencsér, A. Brown Carbon Absorption in the Red and Near-Infrared Spectral Region. *Atmospheric Measurement Techniques* **2017**, *10* (6), 2353–2359.
- (30) Pandey, A.; Hsu, A.; Tiwari, S.; Pervez, S.; Chakrabarty, R. K. Light Absorption by Organic Aerosol Emissions Rivals That of Black Carbon from Residential Biomass Fuels in South Asia. *Environ. Sci. Technol. Lett.* **2020**, *7* (4), 266–272.
- (31) Feng, Y.; Ramanathan, V.; Kotamarthi, V. R. Brown Carbon: A Significant Atmospheric Absorber of Solar Radiation? *Atmospheric Chemistry and Physics* **2013**, *13* (17), 8607–8621.
- (32) Jo, D. S.; Park, R. J.; Lee, S.; Kim, S.-W.; Zhang, X. A Global Simulation of Brown Carbon: Implications for Photochemistry and Direct Radiative Effect. *Atmospheric Chemistry and Physics* **2016**, *16* (5), 3413–3432.
- (33) Wang, X.; Heald, C. L.; Ridley, D. A.; Schwarz, J. P.; Spackman, J. R.; Perring, A. E.; Coe, H.; Liu, D.; Clarke, A. D. Exploiting Simultaneous Observational Constraints on Mass and

Absorption to Estimate the Global Direct Radiative Forcing of Black Carbon and Brown Carbon. *Atmospheric Chemistry and Physics* **2014**, *14* (20), 10989–11010.

- (34) Wu, G.; Ram, K.; Fu, P.; Wang, W.; Zhang, Y.; Liu, X.; Stone, E. A.; Pradhan, B. B.; Dangol, P. M.; Panday, A. K.; Wan, X.; Bai, Z.; Kang, S.; Zhang, Q.; Cong, Z. Water-Soluble Brown Carbon in Atmospheric Aerosols from Godavari (Nepal), a Regional Representative of South Asia. *Environ. Sci. Technol.* **2019**, *53* (7), 3471–3479.
- (35) Saleh, R. From Measurements to Models: Toward Accurate Representation of Brown Carbon in Climate Calculations. *Curr Pollution Rep* **2020**, *6* (2), 90–104.
- (36) Zhang, A.; Wang, Y.; Zhang, Y.; Weber, R. J.; Song, Y.; Ke, Z.; Zou, Y. Modeling the Global Radiative Effect of Brown Carbon: A Potentially Larger Heating Source in the Tropical Free Troposphere than Black Carbon. *Atmospheric Chemistry and Physics* **2020**, *20* (4), 1901–1920.
- (37) Adler, G.; Wagner, N. L.; Lamb, K. D.; Manfred, K. M.; Schwarz, J. P.; Franchin, A.; Middlebrook, A. M.; Washenfelder, R. A.; Womack, C. C.; Yokelson, R. J.; Murphy, D. M. Evidence in Biomass Burning Smoke for a Light-Absorbing Aerosol with Properties Intermediate between Brown and Black Carbon. *Aerosol Science and Technology* **2019**, *53* (9), 976–989.
- (38) Cheng, Z.; Atwi, K.; Onyima, T.; Saleh, R. Investigating the Dependence of Light-Absorption Properties of Combustion Carbonaceous Aerosols on Combustion Conditions. *Aerosol Science and Technology* **2019**, *53* (4), 419–434.
- (39) Sun, H.; Biedermann, L.; Bond, T. C. Color of Brown Carbon: A Model for Ultraviolet and Visible Light Absorption by Organic Carbon Aerosol. *Geophysical Research Letters* **2007**, *34* (17).
- (40) Chen, Y.; Bond, T. C. Light Absorption by Organic Carbon from Wood Combustion. *Atmospheric Chemistry and Physics* **2010**, *10* (4), 1773–1787.
- (41) Sun, J.; Zhi, G.; Hitzenberger, R.; Chen, Y.; Tian, C.; Zhang, Y.; Feng, Y.; Cheng, M.; Zhang, Y.; Cai, J.; Chen, F.; Qiu, Y.; Jiang, Z.; Li, J.; Zhang, G.; Mo, Y. Emission Factors and Light Absorption Properties of Brown Carbon from Household Coal Combustion in China. *Atmospheric Chemistry and Physics* **2017**, *17* (7), 4769–4780.
- (42) Wang, Y.; Hu, M.; Xu, N.; Qin, Y.; Wu, Z.; Zeng, L.; Huang, X.; He, L. Chemical Composition and Light Absorption of Carbonaceous Aerosols Emitted from Crop Residue Burning: Influence of Combustion Efficiency. *Atmospheric Chemistry and Physics* **2020**, *20*, 13721–13734.
- (43) Huang, S.; Feng, H.; Zuo, S.; Liao, J.; He, M.; Shima, M.; Tamura, K.; Li, Y.; Ma, L. Short-Term Effects of Carbonaceous Components in PM_{2.5} on Pulmonary Function: A Panel Study of 37 Chinese Healthy Adults. *Int J Environ Res Public Health* **2019**, *16* (13), 2259.

- (44) Yan, J.; Wang, X.; Gong, P.; Wang, C.; Cong, Z. Review of Brown Carbon Aerosols: Recent Progress and Perspectives. *Science of The Total Environment* **2018**, *634*, 1475–1485.
- (45) Koistinen, K. J.; Hänninen, O.; Rotko, T.; Edwards, R. D.; Moschandreas, D.; Jantunen, M. J. Behavioral and Environmental Determinants of Personal Exposures to PM_{2.5} in EXPOLIS – Helsinki, Finland. *Atmospheric Environment* **2001**, *35* (14), 2473–2481.
- (46) Delgado-Saborit, J. M.; Aquilina, N. J.; Meddings, C.; Baker, S.; Harrison, R. M. Relationship of Personal Exposure to Volatile Organic Compounds to Home, Work and Fixed Site Outdoor Concentrations. *Sci Total Environ* **2011**, *409* (3), 478–488. <https://doi.org/10.1016/j.scitotenv.2010.10.014>.
- (47) Scapellato, M. L.; Canova, C.; de Simone, A.; Carrieri, M.; Maestrelli, P.; Simonato, L.; Bartolucci, G. B. Personal PM₁₀ Exposure in Asthmatic Adults in Padova, Italy: Seasonal Variability and Factors Affecting Individual Concentrations of Particulate Matter. *Int J Hyg Environ Health* **2009**, *212* (6), 626–636.
- (48) Shen, G.; Yang, Y.; Wang, W.; Tao, S.; Zhu, C.; Min, Y.; Xue, M.; Ding, J.; Wang, B.; Wang, R.; Shen, H.; Li, W.; Wang, X.; Russell, A. G. Emission Factors of Particulate Matter and Elemental Carbon for Crop Residues and Coals Burned in Typical Household Stoves in China. *Environ Sci Technol* **2010**, *44* (18), 7157–7162.
- (49) Grieshop, A. P.; Marshall, J. D.; Kandlikar, M. Health and Climate Benefits of Cookstove Replacement Options. *Energy Policy* **2011**, *39* (12), 7530–7542.
- (50) *Burning Opportunity: Clean household energy for health, sustainable development and the wellbeing of women and children*. Climate & Clean Air Coalition. (accessed 2022-09-28).
- (51) Brauer, M.; Bartlett, K.; Regalado-Pineda, J.; Perez-Padilla, R. Assessment of Particulate Concentrations from Domestic Biomass Combustion in Rural Mexico. *Environ. Sci. Technol.* **1996**, *30* (1), 104–109.
- (52) *GBD Compare*. Institute for Health Metrics and Evaluation. <http://vizhub.healthdata.org/gbd-compare> (accessed 2023-01-22).
- (53) *United Nations Foundation*. Clean Cooking Alliance. <https://cleancooking.org/sector-directory/united-nations-foundation/> (accessed 2023-01-23).
- (54) Grieshop, A. P.; Marshall, J. D.; Kandlikar, M. Health and Climate Benefits of Cookstove Replacement Options. *Energy Policy* **2011**, *39* (12), 7530–7542.
- (55) Kirchstetter, T. W.; Novakov, T.; Hobbs, P. V. Evidence That the Spectral Dependence of Light Absorption by Aerosols Is Affected by Organic Carbon. *Journal of Geophysical Research: Atmospheres* **2004**, *109* (D21).
- (56) Martinsson, J.; Eriksson, A. C.; Nielsen, I. E.; Malmberg, V. B.; Ahlberg, E.; Andersen, C.; Lindgren, R.; Nyström, R.; Nordin, E. Z.; Brune, W. H.; Svenningsson, B.; Swietlicki, E.; Boman, C.; Pagels, J. H. Impacts of Combustion Conditions and Photochemical Processing

- on the Light Absorption of Biomass Combustion Aerosol. *Environ. Sci. Technol.* **2015**, *49* (24), 14663–14671.
- (57) Saleh, R.; Hennigan, C. J.; McMeeking, G. R.; Chuang, W. K.; Robinson, E. S.; Coe, H.; Donahue, N. M.; Robinson, A. L. Absorptivity of Brown Carbon in Fresh and Photo-Chemically Aged Biomass-Burning Emissions. *Atmospheric Chemistry and Physics* **2013**, *13* (15), 7683–7693.
- (58) Rajagopalan, S.; Brook, R. D. The Indoor-Outdoor Air-Pollution Continuum and the Burden of Cardiovascular Disease: An Opportunity for Improving Global Health. *Glob Heart* **2012**, *7* (3), 207–213.
- (59) *Household air pollution*. <https://www.who.int/news-room/fact-sheets/detail/household-air-pollution-and-health> (accessed 2023-01-22).
- (60) Bailis, P. R.; Ogle, D.; MacCarty, N.; Smith, K. R.; Edwards, R. The Water Boiling Test (WBT). 38.
- (61) Cheng, Y.; Lee, S. C.; Ho, K. F.; Fung, K. Positive Sampling Artifacts in Particulate Organic Carbon Measurements in Roadside Environment. *Environ Monit Assess* **2010**, *168* (1), 645–656.
- (62) Watson, J. G.; Chow, J. C.; Chen, L.-W. A.; Frank, N. H. Methods to Assess Carbonaceous Aerosol Sampling Artifacts for IMPROVE and Other Long-Term Networks. *Journal of the Air & Waste Management Association* **2009**, *59* (8), 898–911.
- (63) Birch, M. E.; Cary, R. A. Elemental Carbon-Based Method for Monitoring Occupational Exposures to Particulate Diesel Exhaust. *Aerosol Science and Technology* **1996**, *25* (3), 221–241.
- (64) Chow, J. C.; Watson, J. G.; Pritchett, L. C.; Pierson, W. R.; Frazier, C. A.; Purcell, R. G. The Dri Thermal/Optical Reflectance Carbon Analysis System: Description, Evaluation and Applications in U.S. Air Quality Studies. *Atmospheric Environment. Part A. General Topics* **1993**, *27* (8), 1185–1201.
- (65) Wong, J. P. S.; Nenes, A.; Weber, R. J. Changes in Light Absorptivity of Molecular Weight Separated Brown Carbon Due to Photolytic Aging. *Environ. Sci. Technol.* **2017**, *51* (15), 8414–8421.
- (66) Wong, J. P. S.; Tsagkarakaki, M.; Tsiotra, I.; Mihalopoulos, N.; Violaki, K.; Kanakidou, M.; Sciare, J.; Nenes, A.; Weber, R. J. Atmospheric Evolution of Molecular-Weight-Separated Brown Carbon from Biomass Burning. *Atmospheric Chemistry and Physics* **2019**, *19* (11), 7319–7334.
- (67) Hecobian, A.; Zhang, X.; Zheng, M.; Frank, N.; Edgerton, E. S.; Weber, R. J. Water-Soluble Organic Aerosol Material and the Light-Absorption Characteristics of Aqueous Extracts Measured over the Southeastern United States. *Atmos. Chem. Phys.* **2010**, *10* (13), 5965–5977.

- (68) Xie, M.; Shen, G.; Holder, A. L.; Hays, M. D.; Jetter, J. J. Light Absorption of Organic Carbon Emitted from Burning Wood, Charcoal, and Kerosene in Household Cookstoves. *Environ Pollut* **2018**, *240*, 60–67.
- (69) Pratiti, R. Household Air Pollution Related to Biomass Cook Stove Emissions and Its Interaction with Improved Cookstoves. *AIMS Public Health* **2021**, *8* (2), 309–321.
- (70) Isenor, B. Oxidative Potential of Aerosol Emitted from Traditional vs. Improved Cookstoves, Mount Allison University, 2022.
- (71) Pandey, A.; Pervez, S.; Chakrabarty, R. K. Filter-Based Measurements of UV–Vis Mass Absorption Cross Sections of Organic Carbon Aerosol from Residential Biomass Combustion: Preliminary Findings and Sources of Uncertainty. *Journal of Quantitative Spectroscopy and Radiative Transfer* **2016**, *182*, 296–304.
- (72) June, N.; Wang, X.; Chen, L.-W. A.; Chow, J. C.; Watson, J. G.; Wang, X.; Henderson, B. H.; Zheng, Y.; Mao, J. Spatial and Temporal Variability of Brown Carbon in United States: Implications for Direct Radiative Effects. *Geophys Res Lett* **2020**, *47* (23), 10.1029/2020gl090332.
- (73) Christian, T. J.; Kleiss, B.; Yokelson, R. J.; Holzinger, R.; Crutzen, P. J.; Hao, W. M.; Saharjo, B. H.; Ward, D. E. Comprehensive Laboratory Measurements of Biomass-Burning Emissions: 1. Emissions from Indonesian, African, and Other Fuels. *Journal of Geophysical Research: Atmospheres* **2003**, *108* (D23).
- (74) Laskin, A.; Laskin, J.; Nizkorodov, S. A. Chemistry of Atmospheric Brown Carbon. *Chem. Rev.* **2015**, *115* (10), 4335–4382.
- (75) Hecobian, A.; Zhang, X.; Zheng, M.; Frank, N.; Edgerton, E. S.; Weber, R. J. Water-Soluble Organic Aerosol Material and the Light-Absorption Characteristics of Aqueous Extracts Measured over the Southeastern United States. *Atmospheric Chemistry and Physics* **2010**, *10* (13), 5965–5977.
- (76) Atwi, K.; Cheng, Z.; El Hajj, O.; Perrie, C.; Saleh, R. A Dominant Contribution to Light Absorption by Methanol-Insoluble Brown Carbon Produced in the Combustion of Biomass Fuels Typically Consumed in Wildland Fires in the United States. *Environ. Sci.: Atmos.* **2022**, *2* (2), 182–191.
- (77) Wang, Y.; Hu, M.; Xu, N.; Qin, Y.; Wu, Z.; Zeng, L.; Huang, X.; He, L. Chemical Composition and Light Absorption of Carbonaceous Aerosols Emitted from Crop Residue Burning: Influence of Combustion Efficiency. *Atmospheric Chemistry & Physics* **2020**, *20*, 13721–13734.
- (78) Choudhary, V.; Singh, G. K.; Gupta, T.; Paul, D. Absorption and Radiative Characteristics of Brown Carbon Aerosols during Crop Residue Burning in the Source Region of Indo-Gangetic Plain. *Atmospheric Research* **2021**, *249*, 105285.

- (79) Choudhary, V.; Roson, M. L.; Guo, X.; Gautam, T.; Gupta, T.; Zhao, R. Aqueous-Phase Photochemical Oxidation of Water-Soluble Brown Carbon Aerosols Arising from Solid Biomass Fuel Burning. *Environ. Sci.: Atmos.* **2023**.
- (80) Hettiyadura, A. P. S.; Garcia, V.; Li, C.; West, C. P.; Tomlin, J.; He, Q.; Rudich, Y.; Laskin, A. Chemical Composition and Molecular-Specific Optical Properties of Atmospheric Brown Carbon Associated with Biomass Burning. *Environ. Sci. Technol.* **2021**, *55* (4), 2511–2521.
- (81) Liu, J.; Bergin, M.; Guo, H.; King, L.; Kotra, N.; Edgerton, E.; Weber, R. J. Size-Resolved Measurements of Brown Carbon in Water and Methanol Extracts and Estimates of Their Contribution to Ambient Fine-Particle Light Absorption. *Atmospheric Chemistry and Physics* **2013**, *13* (24), 12389–12404.
- (82) XingJun, F.; MeiJu, L.; Tao, C.; ChongChong, C.; FeiYue, L.; Yue, X.; SiYe, W.; JianZhong, S.; Ping'an, P. Optical Properties and Oxidative Potential of Water- and Alkaline-Soluble Brown Carbon in Smoke Particles Emitted from Laboratory Simulated Biomass Burning. *Atmospheric Environment* **2018**, *194*, 48–57.
- (83) Hellén, H.; Kangas, L.; Kousa, A.; Vestenius, M.; Teinilä, K.; Karppinen, A.; Niemi, J. V. Evaluation of the Impact of Wood Combustion on Benzo(a)Pyrene (BaP) Concentrations; Ambient Measurements and Dispersion Modelling in Helsinki, Finland.
- (84) Kistler, M.; Schmidl, C.; Wagner, L. S. C.; Lohninger, H.; Kasper-Giebl, A.; Puxbaum, H. Benzo(a)Pyrene Emitted during Small-Scale Wood Burning.
- (85) Bukowska, B.; Mokra, K.; Michałowicz, J. Benzo[a]Pyrene—Environmental Occurrence, Human Exposure, and Mechanisms of Toxicity. *Int J Mol Sci* **2022**, *23* (11), 6348.
- (86) Dong, S.; Wang, S.; Stewart, G.; Hwang, H.-M.; Fu, P. P. N.; Yu, H. Effect of Organic Solvents and Biologically Relevant Ions on the Light-Induced DNA Cleavage by Pyrene and Its Amino and Hydroxy Derivatives. *International Journal of Molecular Sciences* **2002**, *3* (9), 937–947.
- (87) Barry, N. P. E.; Therrien, B. Chapter 13 - Pyrene: The Guest of Honor. In *Organic Nanoreactors*; Sadjadi, S., Ed.; Academic Press: Boston, 2016; pp 421–461.
- (88) Tropp, J.; Ihde, M. H.; Williams, A. K.; White, N. J.; Eedugurala, N.; Bell, N. C.; Azoulay, J. D.; Bonizzoni, M. A Sensor Array for the Discrimination of Polycyclic Aromatic Hydrocarbons Using Conjugated Polymers and the Inner Filter Effect. *Chem. Sci.* **2019**, *10* (44), 10247–10255.
- (89) Li, S.; Jiang, X.; Roveretto, M.; George, C.; Liu, L.; Jiang, W.; Zhang, Q.; Wang, W.; Ge, M.; Du, L. Photochemical Aging of Atmospherically Reactive Organic Compounds Involving Brown Carbon at the Air–Aqueous Interface. *Atmos. Chem. Phys.* **2019**, *19* (15), 9887–9902.
- (90) Li, J.; Zhang, Q.; Wang, G.; Li, J.; Wu, C.; Liu, L.; Wang, J.; Jiang, W.; Li, L.; Ho, K. F.; Cao, J. Optical Properties and Molecular Compositions of Water-Soluble and Water-

Insoluble Brown Carbon (BrC) Aerosols in Northwest China. *Atmospheric Chemistry and Physics* **2020**, *20* (8), 4889–4904.

- (91) Dasari, S.; Andersson, A.; Bikkina, S.; Holmstrand, H.; Budhavant, K.; Satheesh, S.; Asmi, E.; Kesti, J.; Backman, J.; Salam, A.; Bisht, D. S.; Tiwari, S.; Hameed, Z.; Gustafsson, Ö. Photochemical Degradation Affects the Light Absorption of Water-Soluble Brown Carbon in the South Asian Outflow. *Science Advances* **2019**, *5* (1), eaau8066.
- (92) Gao, D.; Ripley, S.; Weichenthal, S.; Godri Pollitt, K. J. Ambient Particulate Matter Oxidative Potential: Chemical Determinants, Associated Health Effects, and Strategies for Risk Management. *Free Radical Biology and Medicine* **2020**, *151*, 7–25.

Appendix

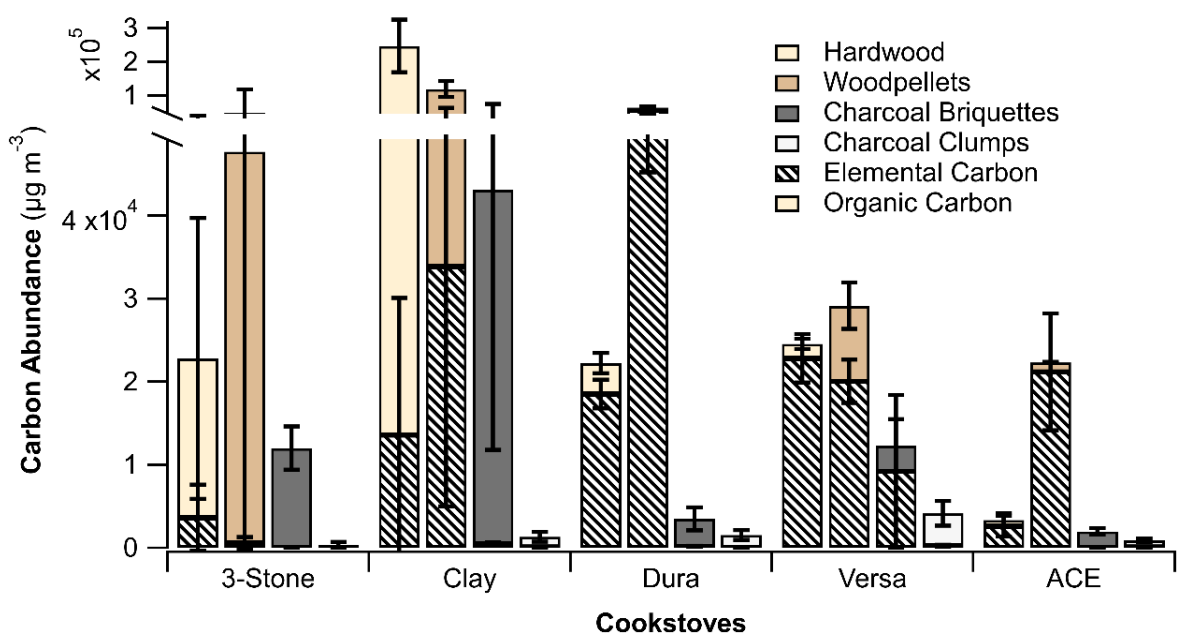


Figure A1. Carbon abundance ($\mu\text{g m}^{-3}$) of elemental (dashed) and organic carbon (solid) for all 20 fuel-cookstove combinations. Error bars represent ± 1 standard deviation ($n=3$).

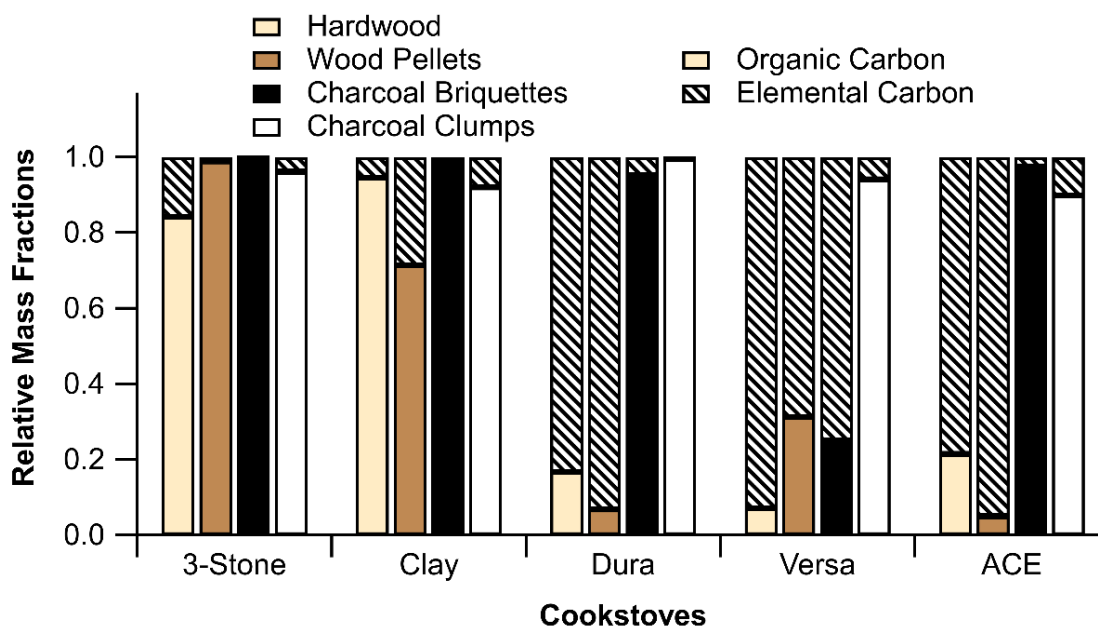


Figure A2. Relative mass fractions of elemental (dashed) and organic carbon (solid) for all 20 fuel-cookstove combinations.

Table A1. Average absorption coefficients (m^{-1}) at 365, 400, 450, 520, 590, and 660 nm for MS–BrC emitted from all 20 fuel–cookstove combinations. Standard deviations are also shown.

Cooking Method	$b_{\text{abs}_{365}}$ (m^{-1})	$b_{\text{abs}_{400}}$ (m^{-1})	$b_{\text{abs}_{450}}$ (m^{-1})	$b_{\text{abs}_{520}}$ (m^{-1})	$b_{\text{abs}_{590}}$ (m^{-1})	$b_{\text{abs}_{660}}$ (m^{-1})
3–stone + hardwood	3.9 ± 1.5 $\times 10^{-4}$	19 ± 6.2 $\times 10^{-5}$	0.8 ± 2.2 $\times 10^{-4}$	27 ± 6.1 $\times 10^{-6}$	91 ± 9.3 $\times 10^{-7}$	5.2 ± 1.5 $\times 10^{-6}$
3–stone + wood pellets	10 ± 7.6 $\times 10^{-4}$	4.6 ± 3.2 $\times 10^{-4}$	1.8 ± 1.3 $\times 10^{-4}$	5.9 ± 3.8 $\times 10^{-5}$	2.6 ± 1.5 $\times 10^{-5}$	11 ± 8.9 $\times 10^{-6}$
3–stone + briquettes	26 ± 7.5 $\times 10^{-5}$	13 ± 3.5 $\times 10^{-5}$	4.9 ± 1.3 $\times 10^{-5}$	13 ± 2.2 $\times 10^{-6}$	37 ± 7.5 $\times 10^{-7}$	11 ± 8.6 $\times 10^{-7}$
3–stone + clumps	10 ± 5.1 $\times 10^{-6}$	6.5 ± 2.9 $\times 10^{-6}$	3.3 ± 1.5 $\times 10^{-6}$	11 ± 6.3 $\times 10^{-7}$	4.8 ± 3.0 $\times 10^{-7}$	2.2 ± 1.7 $\times 10^{-7}$
Clay + hardwood	5.7 ± 1.2 $\times 10^{-3}$	27 ± 6.4 $\times 10^{-4}$	11 ± 2.9 $\times 10^{-4}$	3.1 ± 1.1 $\times 10^{-4}$	11 ± 8.4 $\times 10^{-5}$	4.9 ± 3.2 $\times 10^{-5}$
Clay + wood pellets	2.9 ± 1.1 $\times 10^{-3}$	16 ± 6.5 $\times 10^{-4}$	6.5 ± 2.9 $\times 10^{-4}$	20 ± 8.1 $\times 10^{-5}$	7.5 ± 2.8 $\times 10^{-5}$	3.7 ± 1.6 $\times 10^{-5}$
Clay + briquettes	5.7 ± 1.6 $\times 10^{-4}$	31 ± 8.7 $\times 10^{-5}$	11 ± 2.5 $\times 10^{-5}$	34 ± 4.5 $\times 10^{-6}$	130 ± 3.2 $\times 10^{-7}$	46 ± 8.5 $\times 10^{-7}$
Clay + clumps	3.6 ± 2.1 $\times 10^{-5}$	2.3 ± 1.3 $\times 10^{-5}$	13 ± 7.6 $\times 10^{-6}$	5.2 ± 3.2 $\times 10^{-6}$	2.6 ± 1.6 $\times 10^{-6}$	13 ± 9.5 $\times 10^{-7}$
Dura + hardwood	20 ± 6.1 $\times 10^{-5}$	12 ± 4.4 $\times 10^{-5}$	6.3 ± 2.8 $\times 10^{-5}$	3.0 ± 1.8 $\times 10^{-5}$	1.5 ± 1.3 $\times 10^{-5}$	7.9 ± 6.4 $\times 10^{-6}$
Dura + wood pellets	50 ± 3.3 $\times 10^{-5}$	34 ± 4.1 $\times 10^{-5}$	19 ± 3.0 $\times 10^{-5}$	10 ± 1.9 $\times 10^{-5}$	68 ± 9.7 $\times 10^{-6}$	35 ± 8.3 $\times 10^{-6}$
Dura + briquettes	10 ± 1.4 $\times 10^{-5}$	63 ± 8.7 $\times 10^{-6}$	30 ± 4.2 $\times 10^{-6}$	13 ± 2.8 $\times 10^{-6}$	6.5 ± 2.5 $\times 10^{-6}$	3.1 ± 1.3 $\times 10^{-6}$
Dura + clumps	8.4 ± 2.6 $\times 10^{-6}$	6.3 ± 1.6 $\times 10^{-6}$	35 ± 8.9 $\times 10^{-7}$	7.3 ± 4.4 $\times 10^{-7}$	4.4 ± 4.4 $\times 10^{-7}$	2.4 ± 2.8 $\times 10^{-7}$
Versa + hardwood	4.7 ± 2.2 $\times 10^{-5}$	2.9 ± 1.5 $\times 10^{-5}$	13 ± 7.3 $\times 10^{-6}$	4.9 ± 3.1 $\times 10^{-6}$	2.5 ± 1.6 $\times 10^{-6}$	1.2 ± 1.0 $\times 10^{-6}$
Versa + wood pellets	3.5 ± 2.0 $\times 10^{-4}$	2.0 ± 1.1 $\times 10^{-4}$	9.0 ± 4.9 $\times 10^{-5}$	3.4 ± 1.7 $\times 10^{-5}$	1.7 ± 1.1 $\times 10^{-5}$	9.6 ± 7.6 $\times 10^{-6}$

Cooking Method	b_{abs_365} (m⁻¹)	b_{abs_400} (m⁻¹)	b_{abs_450} (m⁻¹)	b_{abs_520} (m⁻¹)	b_{abs_590} (m⁻¹)	b_{abs_660} (m⁻¹)
Versa + briquettes	4.1 ± 2.4 $\times 10^{-4}$	2.3 ± 1.3 $\times 10^{-4}$	8.7 ± 4.9 $\times 10^{-5}$	2.4 ± 1.5 $\times 10^{-5}$	11 ± 8.5 $\times 10^{-6}$	4.5 ± 3.3 $\times 10^{-6}$
Versa + clumps	3.8 ± 1.7 $\times 10^{-5}$	2.9 ± 1.1 $\times 10^{-5}$	16 ± 6.0 $\times 10^{-6}$	4.0 ± 2.5 $\times 10^{-6}$	1.8 ± 1.4 $\times 10^{-6}$	7.1 ± 6.3 $\times 10^{-7}$
ACE + hardwood	4.3 ± 2.8 $\times 10^{-5}$	2.5 ± 1.3 $\times 10^{-5}$	13 ± 6.0 $\times 10^{-6}$	5.9 ± 2.8 $\times 10^{-6}$	3.1 ± 1.8 $\times 10^{-6}$	1.7 ± 1.1 $\times 10^{-6}$
ACE + wood pellets	22 ± 5.2 $\times 10^{-6}$	12 ± 3.2 $\times 10^{-6}$	4.4 ± 1.8 $\times 10^{-6}$	14 ± 7.5 $\times 10^{-7}$	7.0 ± 4.5 $\times 10^{-7}$	3.5 ± 3.8 $\times 10^{-7}$
ACE + briquettes	7.4 ± 1.7 $\times 10^{-5}$	4.4 ± 1.1 $\times 10^{-5}$	19 ± 4.9 $\times 10^{-6}$	7.3 ± 2.3 $\times 10^{-6}$	30 ± 9.9 $\times 10^{-7}$	14 ± 5.5 $\times 10^{-7}$
ACE + clumps	13 ± 4.3 $\times 10^{-6}$	8.8 ± 3.0 $\times 10^{-6}$	5.3 ± 1.9 $\times 10^{-6}$	23 ± 8.5 $\times 10^{-7}$	13 ± 6.5 $\times 10^{-7}$	6.1 ± 2.9 $\times 10^{-7}$

Table A2. Average absorption coefficients (m^{-1}) at 365, 400, 450, 520, 590, and 660 nm for WS–BrC emitted from all 20 fuel–cookstove combinations. Standard deviations are also shown.

Cooking Method	b_{abs_365} (m^{-1})	b_{abs_400} (m^{-1})	b_{abs_450} (m^{-1})	b_{abs_520} (m^{-1})	b_{abs_590} (m^{-1})	b_{abs_660} (m^{-1})
3–stone + hardwood	15 ± 6.5 $\times 10^{-5}$	4.5 ± 1.6 $\times 10^{-5}$	16 ± 6.4 $\times 10^{-6}$	9.9 ± 7.0 $\times 10^{-6}$	7.1 ± 7.1 $\times 10^{-6}$	1.5 ± 1.8 $\times 10^{-6}$
3–stone + wood pellets	7.0 ± 2.5 $\times 10^{-4}$	17 ± 4.8 $\times 10^{-5}$	4.4 ± 1.3 $\times 10^{-5}$	1.8 ± 1.0 $\times 10^{-5}$	8.9 ± 6.1 $\times 10^{-6}$	4.4 ± 1.9 $\times 10^{-6}$
3–stone + briquettes	78 ± 8.8 $\times 10^{-6}$	33 ± 3.7 $\times 10^{-6}$	96 ± 6.7 $\times 10^{-7}$	23 ± 1.1 $\times 10^{-7}$	7.4 ± 1.7 $\times 10^{-7}$	3.7 ± 2.8 $\times 10^{-7}$
3–stone + clumps	4.0 ± 1.3 $\times 10^{-6}$	2.9 ± 1.0 $\times 10^{-6}$	19 ± 8.1 $\times 10^{-7}$	5.2 ± 2.4 $\times 10^{-7}$	19 ± 8.7 $\times 10^{-8}$	7.9 ± 3.5 $\times 10^{-8}$
Clay + hardwood	15 ± 5.5 $\times 10^{-4}$	3.3 ± 1.4 $\times 10^{-4}$	6.5 ± 6.6 $\times 10^{-5}$	160 ± 3.0 $\times 10^{-7}$	2.9 ± 7.8 $\times 10^{-5}$	2.0 ± 1.4 $\times 10^{-5}$
Clay + wood pellets	4.7 ± 1.9 $\times 10^{-4}$	15 ± 3.6 $\times 10^{-5}$	43 ± 7.1 $\times 10^{-6}$	10 ± 6.9 $\times 10^{-6}$	9.6 ± 4.2 $\times 10^{-6}$	3.7 ± 3.2 $\times 10^{-6}$
Clay + briquettes	2.5 ± 1.2 $\times 10^{-4}$	14 ± 6.5 $\times 10^{-5}$	41 ± 1.8 $\times 10^{-5}$	8.3 ± 4.4 $\times 10^{-6}$	31 ± 1.6 $\times 10^{-7}$	10 ± 1.3 $\times 10^{-7}$
Clay + clumps	15 ± 6.7 $\times 10^{-6}$	9.6 ± 4.3 $\times 10^{-6}$	6.2 ± 3.0 $\times 10^{-6}$	2.1 ± 1.3 $\times 10^{-6}$	8.0 ± 5.9 $\times 10^{-7}$	2.4 ± 1.1 $\times 10^{-7}$
Dura + hardwood	60 ± 9.8 $\times 10^{-6}$	32 ± 1.8 $\times 10^{-6}$	16 ± 1.7 $\times 10^{-6}$	7.9 ± 1.5 $\times 10^{-6}$	4.1 ± 1.1 $\times 10^{-6}$	22 ± 1.2 $\times 10^{-7}$
Dura + wood pellets	15 ± 9.3 $\times 10^{-5}$	5.3 ± 3.2 $\times 10^{-5}$	2.0 ± 1.2 $\times 10^{-5}$	6.3 ± 4.0 $\times 10^{-6}$	3.3 ± 2.4 $\times 10^{-6}$	7.9 ± 2.0 $\times 10^{-7}$
Dura + briquettes	28 ± 9.3 $\times 10^{-6}$	15 ± 4.8 $\times 10^{-6}$	47 ± 8.8 $\times 10^{-7}$	9.7 ± 2.6 $\times 10^{-7}$	39 ± 4.6 $\times 10^{-8}$	16 ± 4.8 $\times 10^{-8}$
Dura + clumps	7.4 ± 1.9 $\times 10^{-6}$	6.7 ± 2.4 $\times 10^{-6}$	5.0 ± 2.0 $\times 10^{-6}$	8.7 ± 2.7 $\times 10^{-7}$	22 ± 4.8 $\times 10^{-8}$	12 ± 4.3 $\times 10^{-8}$
Versa + hardwood	1.9 ± 1.6 $\times 10^{-5}$	1.3 ± 1.2 $\times 10^{-5}$	8.3 ± 7.6 $\times 10^{-6}$	4.5 ± 4.2 $\times 10^{-6}$	2.6 ± 2.4 $\times 10^{-6}$	1.7 ± 1.7 $\times 10^{-6}$
Versa + wood pellets	6.8 ± 2.8 $\times 10^{-5}$	280 ± 8.5 $\times 10^{-6}$	11 ± 3.8 $\times 10^{-6}$	4.0 ± 1.3 $\times 10^{-6}$	23 ± 9.1 $\times 10^{-7}$	8.6 ± 4.5 $\times 10^{-7}$

Cooking Method	b_{abs_365} (m⁻¹)	b_{abs_400} (m⁻¹)	b_{abs_450} (m⁻¹)	b_{abs_520} (m⁻¹)	b_{abs_590} (m⁻¹)	b_{abs_660} (m⁻¹)
Versa + briquettes	10 ± 7.4 $\times 10^{-6}$	5.9 ± 3.9 $\times 10^{-6}$	2.2 ± 1.2 $\times 10^{-6}$	4.0 ± 2.2 $\times 10^{-6}$	3.4 ± 1.2 $\times 10^{-7}$	4.5 ± 2.9 $\times 10^{-8}$
Versa + clumps	22 ± 6.9 $\times 10^{-6}$	15 ± 3.8 $\times 10^{-6}$	7.9 ± 1.6 $\times 10^{-6}$	17 ± 4.9 $\times 10^{-7}$	6.1 ± 2.3 $\times 10^{-7}$	3.0 ± 2.5 $\times 10^{-7}$
ACE + hardwood	2.0 ± 1.3 $\times 10^{-5}$	10 ± 5.6 $\times 10^{-6}$	5.7 ± 3.1 $\times 10^{-6}$	3.2 ± 1.9 $\times 10^{-6}$	2.0 ± 1.2 $\times 10^{-6}$	8.9 ± 5.5 $\times 10^{-7}$
ACE + wood pellets	9.2 ± 2.5 $\times 10^{-6}$	5.8 ± 2.0 $\times 10^{-6}$	3.0 ± 1.3 $\times 10^{-6}$	12 ± 4.8 $\times 10^{-7}$	8.0 ± 4.7 $\times 10^{-7}$	4.3 ± 2.1 $\times 10^{-7}$
ACE + briquettes	19 ± 2.3 $\times 10^{-6}$	11 ± 1.5 $\times 10^{-6}$	44 ± 7.8 $\times 10^{-7}$	14 ± 3.7 $\times 10^{-7}$	6.0 ± 1.6 $\times 10^{-7}$	2.5 ± 1.3 $\times 10^{-7}$
ACE + clumps	7.9 ± 2.5 $\times 10^{-6}$	5.6 ± 1.8 $\times 10^{-6}$	3.7 ± 1.3 $\times 10^{-6}$	16 ± 7.1 $\times 10^{-7}$	8.0 ± 4.3 $\times 10^{-7}$	4.0 ± 2.4 $\times 10^{-7}$

